ACS Sustainable Chemistry & Engineering

Research Article

Cite This: ACS Sustainable Chem. Eng. 2019, 7, 10516−10532

pubs.acs.org/journal/ascecg

Sustainable Electro-Responsive Semi-Interpenetrating Starch/Ionic Liquid Copolymer Networks for the Controlled Sorption/Release of Biomolecules

Akel F. Kanaan,[†] Madalina M. Barsan,[‡] Christopher M. A. Brett,[‡] Carmen Alvarez-Lorenzo,[§] Angel Concheiro,[§] Hermínio C. de Sousa,*[,†] and Ana M. A. Dias*[,†]

[†]CIEPQPF, Chemical Engineering Department, FCTUC, University of Coimbra, Pólo II, Rua Silvio Lima, 3030-790 Coimbra, Portugal

[‡]Chemistry Department, FCTUC, University of Coimbra, Rua Larga, 3004-535 Coimbra, Portugal

[§]Department of Pharmacology, Pharmacy and Pharmaceutical Technology, R+D Pharma Group (GI-1645), Faculty of Pharmacy, Praza Seminario de Estudos Galegos, s/n. Campus sur, University of Santiago de Compostela, 15782 Santiago de Compostela, Spain

Supporting Information

Downloaded by UNIV OF LIMERICK at 02:18:17:600 on June 25, 2019
from https://pubs.acs.org/doi/10.1021/acssuschemeng.9b01071.

ABSTRACT: The main objective of this work was the development and characterization of sustainable electro-responsive ionic liquid-based cationic copolymers. For this purpose degradable semi-interpenetrating polymer networks (s-IPNs) based on starch and on ion-conducting cationic copolymers of 2-hydroxyethyl methacrylate (HEMA) and 1-butyl-3-vinylimidazolium chloride (BVImCl), cross-linked with *N*,*N*′-methylenebis-(acrylamide) (MBA), were synthesized by following principles of green chemistry. Cross-linked poly(HEMA-*co*-BVImCl) copolymers were also prepared for comparison. The resulting cationic hydrogels (copolymer and s-IPNs) were characterized in terms of their physicochemical, thermomechanical, morphological, and electrochemical properties, as well as in terms of cell viability and proliferation against fibroblast cells. Furthermore, the electro-assisted sorption/release capacity of the prepared hydrogels toward L-tryptophan (used as a model biomolecule) was also studied at different applied DC voltages (0, 2, 5, and 100 V). Results demonstrated that the properties of the synthesized hydrogels can be tuned, depending on their relative chemical composition, presenting electronic conductivity and ionic conductivity values in the 0.1 to 5.2 S cm^{-1} range, and complex shear modulus in the 0.6 to 6.4 MPa range. The sorption/release capacity of the s-IPNs after 3 h at 25 °C can also be modulated between 2.5 and 70% and 4.5 and 40%, depending on the applied DC voltage and/or sorption/release medium. Finally, none of the synthesized cationic hydrogels induced fibroblast cells lysis, although s-IPNs had a lower impact on cell proliferation than poly(HEMA-*co*-BVImCl) copolymers, indicating a favorable effect of starch on the biocompatibility of the synthesized s-IPNs. The designed cationic hydrogels could be useful for the development of efficient, stable, degradable and cheaper soft and multiresponsive platforms with potential applications in bioseparation processes, wastewater treatment systems (e.g., pharmaceutical), biomedical devices (e.g., sustained delivery of specific charged-biomolecules), and nonleaching electrochemical devices.

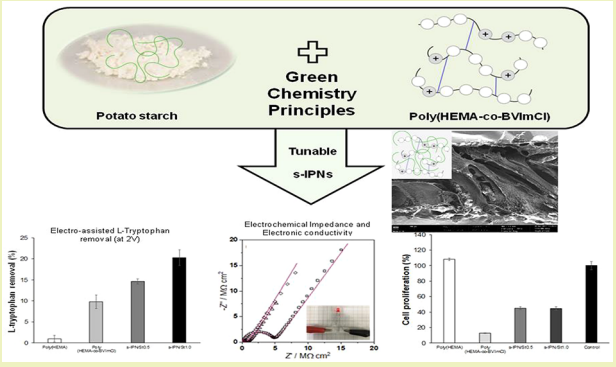

KEYWORDS: *Semi-interpenetrating polymer networks, Starch, Polymerizable imidazolium-based ionic liquids, L-Tryptophan, Electro-assisted sorption/release, Electric stimuli-responsive hydrogel*

INTRODUCTION

Stimuli-responsive hydrogels, also called "smart" hydrogels, are defined as hydrophilic three-dimensional cross-linked networks that are able to absorb high amounts of water and to respond to different external or internal applied stimuli (e.g., ionic strength, pH, temperature, light and electrical field) through changes in their structures (e.g., swelling, shrinking and/or bending).[1] In recent years much effort has been made to engineer smart multiresponsive hydrogels presenting improved functionalities such as fast response to the applied stimulus, high mechanical stability, biodegradability, biocompatibility and low cost.[2−4]

Biocompatible electrically responsive hydrogels represent an interesting subclass of stimuli-responsive materials since they present narrow and precise response under fine and tunable control of the applied stimuli, e.g. intensity, orientation and

Received: February 22, 2019
Revised: April 24, 2019
Published: May 15, 2019

© 2019 American Chemical Society

DOI: 10.1021/acssuschemeng.9b01071
ACS Sustainable Chem. Eng. 2019, 7, 10516−10532

duration of the applied electrical current.[5,6] These materials may find a broad range of applications in biomedicine, for instance as components of tissue engineering scaffolds, as soft electro-actuators, and as controlled release/sorption systems for bioactive molecules, mostly due to their biocompatibility, soft nature and high water swelling capacity, which make them able to mimic different living tissues.[7−12]

Polyelectrolytes can endow hydrogels with electro-activity relying on ion-conduction mechanisms that result from the interactions between conductive ions and the ionized functional groups present in the polyelectrolyte backbone. In some cases, ion-conductive materials also present electric conductivity in response to an external applied electrical field due to mechanisms not yet completely understood.[13] Examples of natural- and synthetic-based ion-conducting electro-active polyelectrolytes include chitosan and poly(acrylic acid), respectively.[14−17]

Multifunctional tailor-made electro-responsive polyelectrolytes can be successfully obtained through the chain-growth polymerization of vinyl-functionalized ionic liquids.[18] Poly(ionic liquid)s (PILs) combine the properties of monomeric ionic liquids (ILs), such as task-specific design, negligible vapor pressure, broad electrochemical window and high ionic conductivity[19−28] with the mechanical properties of polymers, originating a new subclass of polyelectrolytes which may present promising electro-responsive properties.[19,29−34] Previous studies have shown that the ionic conductivity of PILs is highly influenced, for example, by the cation/anion chemical structure of the IL monomer, by the presence of spacers in PIL's molecular structure and by PIL's molecular weight, structural organization and glass transition temperature.[30,35,36]

The main advantages of using PILs as electro-active hydrogels include the fact that PILs are not pH sensitive polyelectrolytes (i.e., they may stay ionized over broad pH ranges), and they do not require the use of dopants to be electrically active since the ionic conductivity is promoted by the diffusion of the IL counterions (anions or cations depending on the vinyl-functionalized moiety that constitutes the PIL backbone). Nevertheless, the application of PILs is hampered in low ionic strength aqueous solutions since these materials usually behave as superabsorbent hydrogels, due to their high intrinsic charge density, leading to significant loss of mechanical and structural/morphological stability. Moreover, important issues such as PILs biocompatibility and biodegradability have been almost completely neglected so far.

The development of IL-based copolymers and/or IL-based interpenetrating polymer networks (IPNs) are interesting alternative strategies that can contribute to overcome some of those issues. According to the IUPAC definition, IPNs are polymers comprising two or more networks which are at least partially interlaced on a molecular scale, but not covalently bonded to each other, and cannot be separated unless chemical bonds are broken. When the networks can be separated these materials are known as semi-interpenetrating polymer networks (s-IPNs).[37] IPNs and semi-interpenetrating polymer networks (s-IPNs) allow combining specific properties of different polymer networks (e.g., mechanical resistance, stimuli-responsiveness, biocompatibility, etc.) to obtain a different material presenting improved and/or new task-specific tailored properties.[37−39] PIL-based IPNs and s-IPNs have been recently purposed for the development of matrices for proteins encapsulation,[40] stretchable electronics,[41] actuators and/or electrochromic devices,[42] multistimuli responsive sensors,[43] anion-exchange membranes[44] and gas separation membranes.[45]

The main motivation of this work was the development of more stable, sustainable and cytocompatible electric stimuli-responsive IL-based hydrogels. With this in mind, poly(HEMA-*co*-BVImCl) copolymers, composed of 2-hydroxyethyl methacrylate (HEMA) and by 1-butyl-3-vinylimidazolium chloride (BVImCl) cross-linked with *N*,*N*′-methylenebis(acrylamide) (MBA) and s-IPNs composed of starch (St) and poly(HEMA-*co*-BVImCl) copolymers were synthesized and characterized. The use of poly(HEMA-*co*-BVImCl) instead of poly(BVImCl) aims to improve the mechanical stability of the polycationic hydrogel, while maintaining PIL characteristic properties. Moreover, the comonomer HEMA can be regarded as a spacer that may enhance the ionic conduction of chloride anions through the copolymer matrice, and that also may lead to a decrease of the final cost of the envisaged devices (considering HEMA and BVImCl relative costs). s-IPNs were developed in order to evaluate their potential to tune the properties of the prepared poly(HEMA-*co*-BVImCl) copolymer by incorporating starch, at different relative compositions, in their final structures. The obtained hydrogels were characterized for their swelling capacities in different media, thermomechanical stabilities, ionic/electric conductivities, tunable capacities to remove/release a charged biomolecule from different media, and cytocompatibility with fibroblast cells.

Finally, it is important to refer that an effort was made to synthesize the s-IPNs by following principles of green chemistry. This was accomplished by employing: (i) simple one-pot synthesis procedures at mild conditions, chemically stable and low volatile reactants and water as the reaction solvent; (ii) biodegradable compounds (starch) or compounds that can be degraded originating nontoxic derivatives (HEMA and BVImCl); (iii) small amounts of BVImCl (the functional monomer) in comparison with other IL-based liquid−liquid extraction/separation processes; (iv) small amounts of polymerization catalyst (thermal initiator); and (v) starch (a biodegradable, biocompatible, readily available and cheap renewable feedstock[46−48]) as a strategy to tune the properties of the poly(HEMA-*co*-BVImCl) copolymer. Moreover, the proposed strategy originates hydrogels that present long-term stability in aqueous media, avoiding BVImCl leaching/leakage during usage, and consequently avoiding air/water contamination.

MATERIALS AND METHODS

Materials. Water-soluble potato starch (St); 2-hydroxyethyl methacrylate (HEMA, 97%), *N*,*N*′-methylenebis(acrylamide) (MBA, 99%); 2,2′-azobis (2-methylpropionamidine) dihydrochloride (AIBA, 97%); L-tryptophan (Try, ≥98%) and potassium sulfate (used to create a controlled relative humidity (RH) ≥90% at 25 °C) were obtained from Sigma-Aldrich. The ionic liquid 1-butyl-3-vinylimidazolium chloride (BVImCl, 95%) was acquired from Io-Li-Tec, Germany. For the cells assay, BALB/3T3 clone A31 cells (CCL-163) were obtained from ATCC, Dulbecco's modified Eagle's medium (DMEM)/F12 Ham nutrient mixture and the cell proliferation reagent MTT were obtained from Sigma-Aldrich, while the cytotoxicity detection KitPlus (LDH) was obtained from Roche. Buffer solutions used for the water swelling capacity and/or electrosorption measurements were phosphate buffered saline (PBS, pH = 7.4, I = 0.169 M) from Sigma-Aldrich, a phosphate buffer (PB, pH = 7.14, I = 0.027 M), an acetate buffer (AB, pH = 4.0, I = 0.008 M) and Trizma base buffer (TRIZ, pH = 9.9, $I \approx 0$ M), which were prepared

DOI: 10.1021/acssuschemeng.9b01071
ACS Sustainable Chem. Eng. 2019, 7, 10516−10532

Table 1. Feed Compositions and Elemental Analyses of the Hydrogels Synthesized in Aqueous Media (6.44 mL)[a]

Hydrogels	Code	St (mg)	HEMA (mmol)	BVImCl (mmol)	$BVImCl_{theo}$ (mmol IL/g dry sample)[b]	$BVImCl_{exp}$ (mmol IL/g dry sample)[c]
Poly(HEMA)	poly(HEMA)	–	12.37	–	–	–
Poly(HEMA-*co*-BVImCl)	poly(HEMA-*co*-BVImCl)	–	9.28	3.09	1.717	0.974 ± 0.0978
sIPN_Poly(HEMA-*co*-BVImCl)_0.5%St	s-IPN/St0.5	32.2	9.28	3.09	1.717	0.933 ± 0.1607
sIPN_Poly(HEMA-*co*-BVImCl)_1.0%St	s-IPN/St1.0	64.4	9.28	3.09	1.717	1.082 ± 0.0079

[a]Fixed amounts of cross-linker, *N*,*N*′-methylenebis(acrylamide) (MBA) and of initiator, 2,2′-azobis(2-methylpropionamidine) dihydrochloride (AIBA) were employed for all samples (0.0616 and 0.0247 mmol, respectively). [b]Ratio between the number of moles of BVImCl and the total weight of fed reactants (HEMA+BVImCl+MBA+AIBA). [c]Calculated from elemental analysis data as detailed in Supporting Information (Table S1).

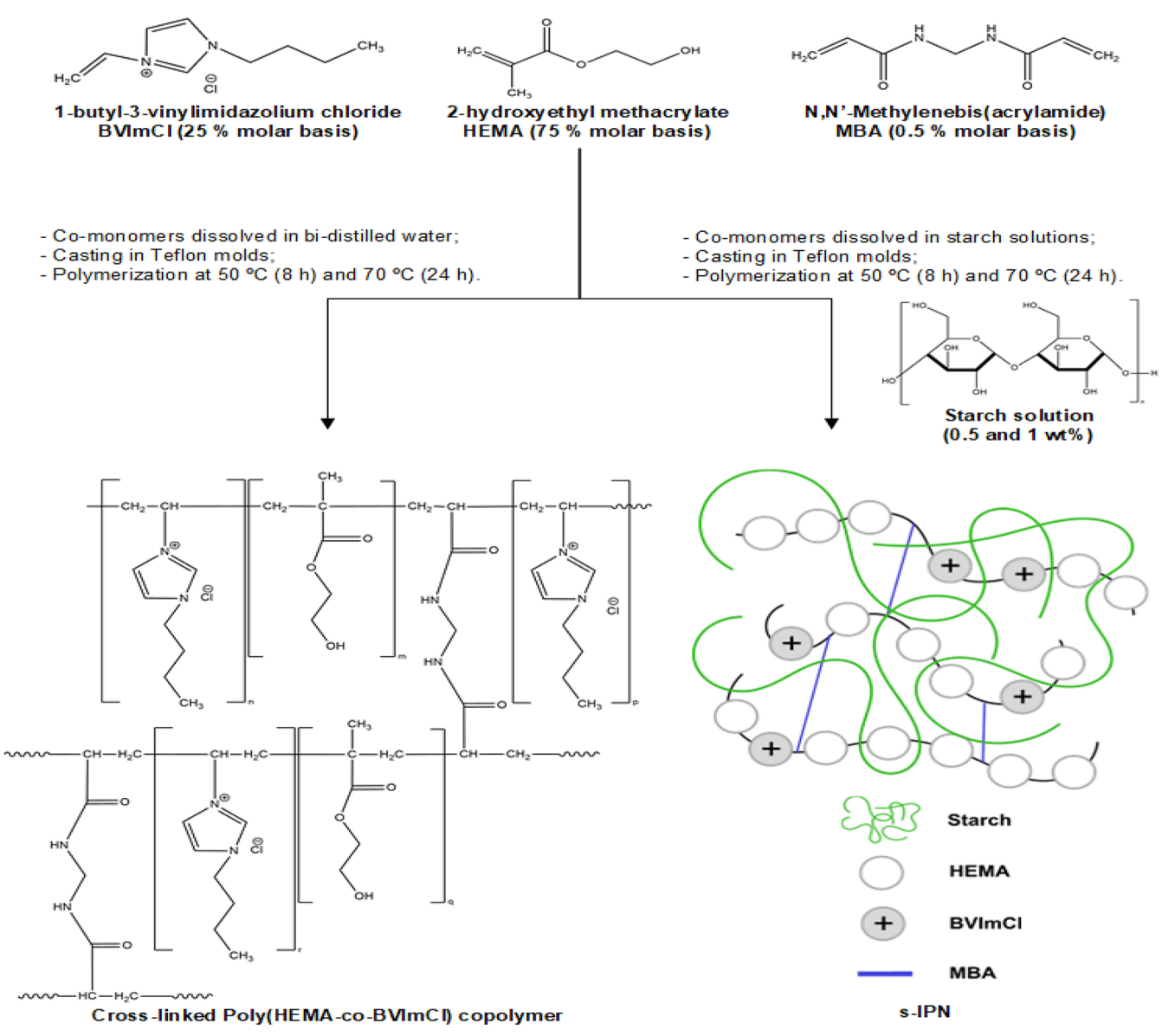

Figure 1. Schematic representation of the hydrogels' chemical structure.

as follows (for 500 mL): (i) PB, 0.31 g of monobasic sodium phosphate (NaH_2PO_4) and 0.52 g of sodium phosphate dibasic (Na_2HPO_4), both from Riedel-de Haen, dissolved in bidistilled water; (ii) AB, 0.07 g of sodium acetate 3-hydrated ($CH_3COONa.3H_2O$) from Panreac and 0.20 mL of acetic acid (CH_3COOH) from Fluka, dissolved in bidistilled water; and (iii) TRIZ, 0.5 g of Trizma base ($NH_2C(CH_2OH)_3$) from Sigma-Aldrich, dissolved in bidistilled water. The final pH of all solutions was measured using a pH meter (Standard pH Meter, Jenway).

Synthesis of s-IPN Hydrogels Based on Starch and Poly(HEMA-*co*-BVImCl). s-IPNs studied in this work resulted from the synthesis of cross-linked poly(HEMA-*co*-BVImCl) copolymers in two aqueous starch solutions (0.5 and 1% w/v). Cross-linked

DOI: 10.1021/acssuschemeng.9b01071
ACS Sustainable Chem. Eng. 2019, 7, 10516−10532

poly(HEMA-*co*-BVImCl) copolymers and the homopolymer poly(HEMA) were also synthesized for comparison purposes (synthesized in the same volume of water used for the starch solutions). Poly(HEMA) presents phase separation during polymerization in aqueous media, depending on the initial HEMA/water ratio.[49] In this work, the chemical composition of the prepared copolymers was chosen to fall in the phase diagram region where macroporous phase-separated hydrogels are formed, assuming that the incorporation of BVImCl into the mixture does not significantly change the typical phase separation behavior observed for poly(HEMA).

Comonomers (HEMA/MBA/BVImCl) were dissolved under stirring for 24 h at room temperature in water to prepare poly(HEMA) and poly(HEMA-*co*-BVImCl), or in starch solutions to prepare s-IPNs. Starch solutions (0.5 and 1.0 wt %) were previously obtained by dissolving starch in bidistilled water at 100 °C for 15 min under stirring to obtain transparent and homogeneous solutions that were then cooled to room temperature. Higher starch concentrations were tested but they were not considered in this work because they originated nonhomogeneous s-IPNs (phase separation visible at naked eye) that presented low mechanical stability, probably due to the higher viscosity that may hinder copolymerization/cross-linking reactions.

Cross-linked poly(HEMA-*co*-BVImCl) was obtained by free radical polymerization using MBA as a cross-linker agent (0.5% on molar basis, relatively to the total number of mole of monomers in solution), and AIBA as a thermal initiator (0.2% on molar basis, relative to the total number of moles of monomers in solution). The above indicated solutions were sonicated for 5 min to remove oxygen and inserted in Teflon squared molds (10 × 10 cm) separated by 2 mm using a silicon spacer. The molds were placed in an oven at 50 °C for 8 h and then at 70 °C for 24 h to ensure complete polymerization. The obtained opaque hydrogels were washed in distilled water (2 L replaced twice a day for 3 days) to remove any unreacted monomers. After washing, half of each sample was oven-dried at 50 °C for 48 h and the other half was freeze-dried (using a freeze drier from Telstar, Lyoquest 85 Plus, Spain) at −80 °C under vacuum (0.1 mPa) for 48 h. The chemical composition and the schematic structure of the cationic hydrogels prepared in this work are presented in Table 1 and Figure 1, respectively. Hydrogel samples were coded as indicated in Table 1 for simplicity.

Characterization of the Hydrogels. *Chemical Analysis.* Attenuated total reflection Fourier transform infrared (FTIR-ATR) spectra were acquired using a spectrophotometer (PerkinElmer, Spectrum Two, U.K.) at 128 scans and 4 cm^{-1} resolution between 400 and 4000 cm^{-1}. Elemental analysis was performed to determine the chemical composition of the prepared samples after synthesis and washing procedures. The analysis was carried out in triplicate for each sample in an elemental analyzer (Fisons Instruments, model EA1108 CHNS-O) by the differential thermal conductivity method.

Morphological Properties. A scanning electron microscope (Jeol, model JSM-530, Japan) coupled with energy dispersive X-ray spectroscopy analysis (Phillips, EDX Genesis, model XL 30) was used to observe the morphology (surface and cross section) of freeze-dried hydrogels, as well as the distribution of BVImCl through the prepared hydrogel matrices (by elemental mapping). Scanning electron microscopy energy dispersive X-ray spectroscopy (SEM-EDX) micrographs were obtained at 10 keV for gold-sputtered samples under an argon atmosphere.

Thermomechanical Properties. The thermal stability of freeze-dried hydrogels was measured using a thermogravimetric analyzer (TA Instruments, Q500, USA). Samples (±10 mg) were dried at 50 °C under vacuum for 24 h before analysis. Measurements were conducted from 25 up to 600 °C at a heating rate of 10 °C/min, under nitrogen atmosphere with a flow rate of 40 mL/min. Samples were also analyzed by differential scanning calorimetry (DSC-Q100 equipment from TA Instruments), applying consecutive heating (from 40 up to 150 °C), cooling (from +150 down to −80 °C), and reheating (from −80 up to +200 °C) runs at 10 °C/min, under nitrogen atmosphere (50 mL/min). Samples (±7 mg) were dried before analysis (by freeze-drying) to remove residual water and then sealed immediately in aluminum pans.

The mechanical performance of freeze-dried hydrogels was accessed using a temperature-controlled stress rheometer (ModelRS1, Haake, Vreden, Germany), with a cylindrical sensor system Z34 DIN connected to a temperature-controlled recirculation bath (Haake Phoenix II). Rheological measurements were performed in oscillatory shear mode at a constant shear stress of 100 Pa, and at a frequency sweep of 0.1−100 rad/s at 25 °C. Samples were kept in bidistilled water for 24 h before measurements. Circular shaped water-swollen discs (2 cm diameter and ±2 mm thickness) were placed between the rotatory and the stationary surfaces separated by a fixed gap of 1.5 mm. The complex shear modulus of the samples was calculated following a procedure previously reported in the literature.[50] Measurements were replicated for each sample (at least twice).

Swelling. The water swelling capacity (WSC) of freeze-dried hydrogels was measured at 25 °C in three different aqueous media, having different pH and ionic strength (I) values, namely bidistilled water; phosphate buffer (I = 0.027 M; pH = 7.0) and phosphate buffered saline (I = 0.169 M; pH = 7.4). Dried samples were weighed and then immersed into 15 mL of each medium. At predefined time intervals, swollen samples were weighed (after removing the excess of surface water using a filter paper) and immersed again into the corresponding medium. This process was repeated at pre-established time intervals of 30 min (for the first 3 h), 1 h (for the following 5 h), once a week (for two months) and again after five months. The pH of each medium was checked during measurements (using a Standard pH meter, Meter Lab). The WSC capacity was calculated as the ratio between the weight of water absorbed at time t and the initial weight of the film (before immersion, t = 0), and the results are presented in terms of $g_{water}/g_{dried\ hydrogel}$.

The water vapor sorption (WVS) capacity of freeze- and oven-dried hydrogels was measured for samples previously dried at 50 °C for 24 h under vacuum (Vacuum oven, J.P. Selecta, s.a.). Samples were placed in Petri dishes and stored at 25 °C in hermetic flasks containing a potassium sulfate saturated solution, to increase the relative humidity (RH) of the flasks up to 90% (at 25 °C). Samples were weighed after 24 h and returned to the RH controlled flask and then weighed again after 48 h to guarantee that WVS equilibrium was attained. The shape and size of the samples after each measurement was monitored using a digital camera. The WVS capacity of the samples was calculated as the ratio between the weight of water absorbed at time t and the initial weight of the freeze- or oven-dried samples, and results are presented in terms of $g_{water}/g_{dried\ hydrogel}$ (%). Both WSC and WVS measurements were performed in duplicate.

Impedance Spectroscopy Measurements. Electrochemical impedance spectroscopy (EIS) experiments were performed using a potentiostat/galvanostat/ZRA, (Gamry Instruments, Reference 600). A root-mean-square (rms) perturbation of 350 mV was applied over a frequency range between 1.0 MHz and 0.1 Hz (ten frequency values per decade), superimposed on a fixed potential difference of 0.10 V between the two electrodes. Freeze-dried and oven-dried samples were cut into a squared shape (1 cm^2) and stored at 90% RH and room temperature for 24 h, before EIS measurements. Samples were then placed between two blocking electrodes (1 cm^2, SS316 steel) in the measurement cell in air. The spectra were fitted using appropriate electrical equivalent circuits (ZView 3.2 software, Scribner Associates Inc., U.S.A.). In this work the constant phase element (CPE) was defined as CPE = $\{(Ci\omega)^{\alpha}\}^{-1}$, where C is a constant, i is the square root of −1, ω is the angular frequency and α is a parameter that varies between 0.5 (for heterogeneous/porous surfaces) and 1.0 (for homogeneous/smooth surfaces), and which reflects the nonuniformity and the surface roughness of the material. The resistivity of the hydrogels (ρ, MΩ cm) was obtained from Z_w while the conductivity (σ, S cm^{-1}) was calculated as the inverse of the resistivity.

Electro-Assisted L-Tryptophan Sorption and Desorption Experiments. Electro-assisted sorption and desorption experiments were performed using a flatbed electrophoresis unit MULTI (Carl Roth, Deutschland) at room temperature (±22 °C) which is composed of a horizontal chamber with adjustable anode and cathode platinum

DOI: 10.1021/acssuschemeng.9b01071
ACS Sustainable Chem. Eng. 2019, 7, 10516−10532

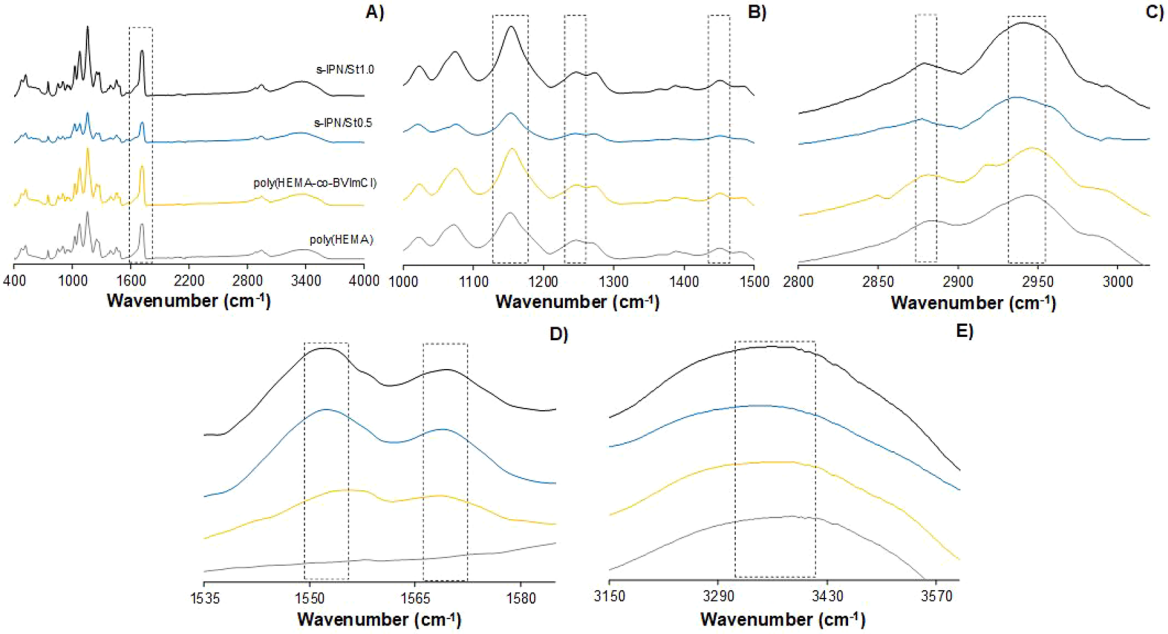

Figure 2. FTIR-ATR spectra of the synthesized hydrogels. Samples are coded as poly(HEMA) (gray), poly(HEMA-*co*-BVImCl) (yellow), s-IPN/St0.5 (blue) and s-IPN/St1.0 (black).

electrodes, and which was connected to an electrophoresis power supply EPS 500/400 (Pharmacia Fine Chemicals, Sweden). Electro-assisted sorption experiments were carried out by placing the electrodes (3 cm apart) over a polystyrene Petri dish containing a fixed volume (~20 mL) of aqueous solutions of the amino acid L-tryptophan (Try) [50.3 mg/mL] dissolved in bidistilled water, TRIZ and AB. Freeze-dried hydrogel samples (±20 mg) were previously hydrated up to equilibrium in bidistilled water (for 24 h) and placed in a midway position between the electrodes. L-Tryptophan (Try) sorption experiments were conducted at different applied voltages (0, 2, 5 and 100 V) for 3 h and in each aqueous media (bidistilled water, TRIZ and AB). The amount of Try removed from each solution by the hydrogels with and without application of an electrical potential was quantified (at 278 nm) using a previously obtained calibration curve of Try in each aqueous media: bidistilled water ([Try] = 0.1981 × Abs, R^2 = 0.998), TRIZ ([Try] = 0.1602 × Abs, R^2 = 0.999) and AB ([Try] = 0.2057 × Abs, R^2 = 0.999). Electro-assisted Try desorption experiments were conducted at different applied voltages (0, 2 and 5 V), for 3 h, and employing the samples that were previously loaded at 2 V. The amount of Try released from the hydrogel was quantified using the calibration curves referred above. Electro-assisted sorption and desorption experiments were conducted at least in duplicate.

Cytocompatibility. Cytocompatibility studies were carried out following the direct contact test (ISO standard 10993-5:2009) using Balb/3T3 cells and by two different assays (cell viability, LDH and cell proliferation, MTT). For both assays, Balb/3T3 cells (20.000 cells/well) were cultured in a 24-well plate for 12 h in Dulbecco's modified Eagle's medium (DMEM)/F12 Ham nutrient mixture (Sigma-Aldrich, USA), supplemented with 10% fetal bovine serum (FBS), 1% L-Glut 200 mM and 1% penicillin (10.000 UI/mL)/streptomycin (10.000 μg/mL) solution, and kept in a humidified atmosphere with 5% CO_2, 90% RH at 37 °C. Freeze-dried hydrogels were cut into pieces of approximately 16 mm^2 and preincubated in culture medium for 24 h. Samples were then sterilized for 30 min with UV radiation (at both sides) and incubated on the cell monolayer for 24 h. The LDH assay was performed by mixing aliquots (100 μL) of the cell culture medium with the reaction medium (100 μL). The positive control (100 μL of medium of lysated cells with Triton X-100) and the negative control (100 μL of medium with no lysozyme cell content) were also mixed with the reaction medium (100 μL). Plates were incubated for 15 min at 15−25 °C, protected from light, and the absorbance at 490 nm was immediately measured in (UV Bio-Rad Model 680 microplate reader, USA). The cell viability was calculated using eq 1):

$$\text{Cell viability (\%)} = \frac{\text{Abs}_{\text{exp}} - \text{Abs}_{\text{negative control}}}{\text{Abs}_{\text{positive control}} - \text{Abs}_{\text{negative control}}} \quad (1)$$

Cell proliferation was measured following the protocol of the Cell Proliferation Kit I (MTT). Briefly, culture medium and samples were removed from wells, and the wells replenished with DMEM/F12 supplemented (250 μL). MTT labeling reagent (25 μL) was added and the plate was maintained at 37 °C, 95% RH and 5% CO_2 for 4 h. The solubilization solution (250 μL) was then added, and the mixture was kept at 35 °C, 95% RH and 5% CO_2 overnight. Finally, the absorbance was recorded at 550 nm (UV Bio-Rad Model 850 microplate reader, USA). Cell proliferation (%) was calculated using eq 2):

$$\text{Cell proliferation (\%)} = \frac{\text{Abs}_{\text{exp}}}{\text{Abs}_{\text{control}}} \times 100 \quad (2)$$

Statistical Analysis. The statistical analysis of the data obtained was performed by the One-way ANOVA test. Statistical significance was considered for *p*-values <0.05.

RESULTS AND DISCUSSION

Structural and Morphological Characterization. The chemical composition of the obtained hydrogels was evaluated by elemental analysis (Table 1) and FTIR-ATR (Figure 2). The presence of the IL (BVImCl) in poly(HEMA-*co*-BVImCl) and s-IPN samples was confirmed by the increase (>2.5 wt %) in the amount of elemental nitrogen (from the imidazolium cation) measured for these samples when compared to poly(HEMA). The small amount of elemental nitrogen measured for poly(HEMA) samples was attributed to the cross-linking agent (MBA) and to the initiator (AIBA). The IL content in all samples (with or without starch) was not statistically different to within 5% and it corresponds to an effective incorporation of BVImCl in the hydrogels of ~0.58 ± 0.045% of the theoretical value (Table 1), as calculated from

DOI: 10.1021/acssuschemeng.9b01071
ACS Sustainable Chem. Eng. 2019, 7, 10516−10532

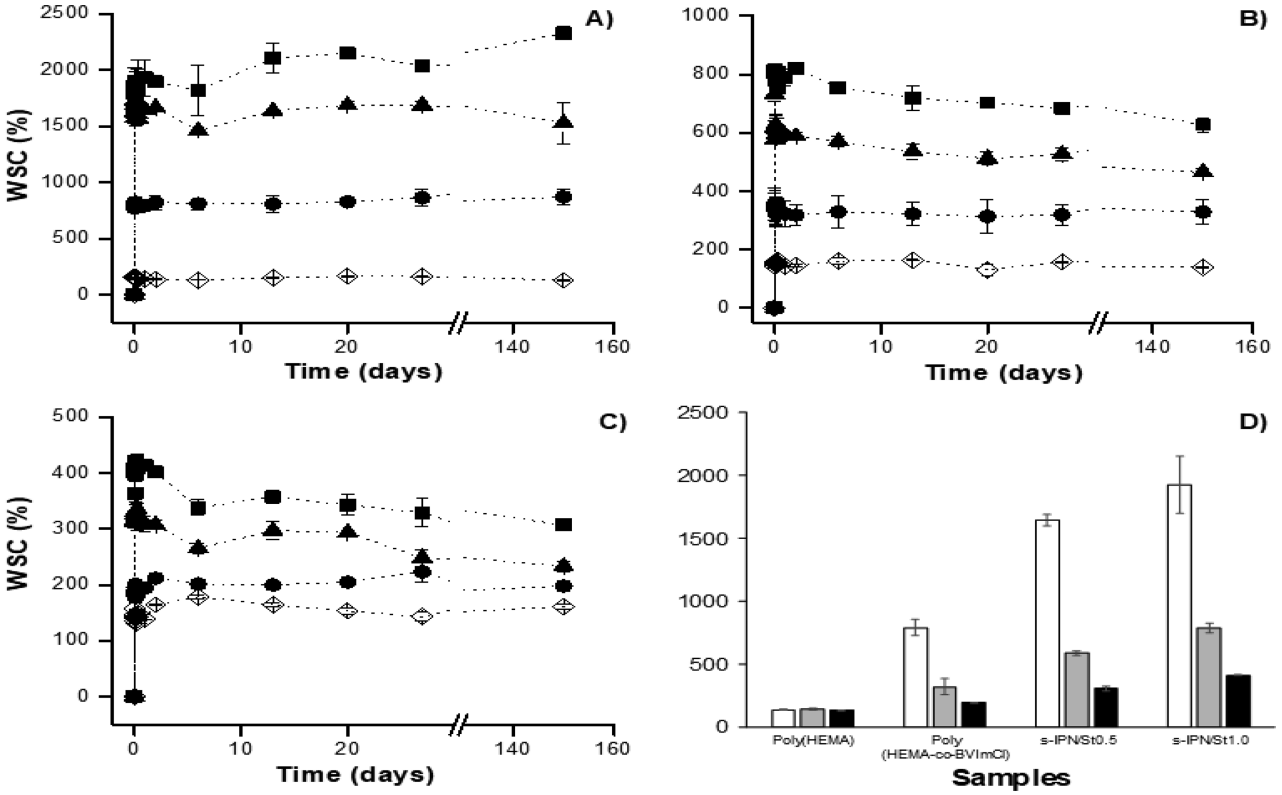

Figure 3. Water sorption capacity (WSC) profiles of the synthesized hydrogels at 25 °C in different aqueous media: (A) bidistilled water, (B) PB and (C) PBS. Symbols represent: poly(HEMA) (◊), poly(HEMA-*co*-BVImCl) (●), s-IPN/St0.5 (▲) and s-IPN/St1.0 (■). (D) Equilibrium water sorption capacity data measured for the hydrogels at 25 °C after 24 h of immersion in different aqueous media: bidistilled water (□), PB (gray ■) and PBS (■).

elemental analysis results (Table S1, Supporting Information). This result may be due to a low reactivity of the IL vinyl monomer, when compared to HEMA (which was not evaluated in this work), and/or IL loss while washing the hydrogels.

The infrared spectra of all samples showed the characteristic peak of HEMA, namely the C═O ester bond at 1707 cm^{-1} (Figure 2A), CH_2 bending, C−O stretching and CH_3 wagging at 1456, 1251 and 1156 cm^{-1}, respectively (Figure 2B) and the C—H stretching vibrations at 2871 and 2945 cm^{-1}[51−53] (Figure 2C). The characteristic peaks of BVImCl in the 1569−1552 cm^{-1} range, assigned to the C═C imidazolium ring vibration,[54,55] were observed in poly(HEMA-*co*-BVImCl) and s-IPN hydrogels (Figure 2D). Additionally, poly(HEMA-*co*-BVImCl) also presented a band at 2918 cm^{-1} which can be assigned to C—H aliphatic stretching of BVImCl.[54] This band was not distinguished for s-IPN because overlapping with the broad bands observed at 2936 and 2944 cm^{-1} due to the C—H stretching of starch[56,57] (Figure 2C). Finally, and when compared to poly(HEMA), a significant shift of 11 cm^{-1} for poly(HEMA-*co*-BVImCl) and of 24.5 cm^{-1} for s-IPNs were observed in the O—H stretch vibration region (3000−3600 cm^{-1}) which may be justified by the higher hygroscopic nature of these samples resulting from their higher hydrophilicity as will be discussed later (Figure 2E). Finally, bands assigned to vinyl vibration of HEMA and BVImCl monomers (1620−1680 cm^{-1})[53,58,59] were not detected in any of the spectra confirming that polymerization has occurred and/or that unreacted monomers were successfully removed from the hydrogels during washing.

The morphology of freeze-dried hydrogels and the elemental mapping of nitrogen and chlorine distribution through the hydrogel structures were analyzed by scanning electron microscopy (SEM) and energy dispersive X-ray spectroscopy (EDX), respectively (Figure S1, Supporting Information). Oven-dried samples were also analyzed by SEM, but all of them revealed compact structures, with no relevant differences among them (data not shown). Hydrogels containing IL, namely for poly(HEMA-*co*-BVImCl) and s-IPNs, presented a macroporous structure with large interconnecting cavities, being clearly different from the globular dense structure of poly(HEMA). As previously discussed in the literature, the observed globular structure of poly(HEMA) results from phase separation that occurs as the water-soluble monomer HEMA is being converted into nonsoluble poly(HEMA).[49] The presence of the IL in the copolymer backbone decreased the original hydrophobicity of poly(HEMA), thus avoiding phase separation. The cationic nature of the hydrogels induced high water sorption capacities that led to the formation of macroporous structures after removing water by freeze-drying. Compared to poly(HEMA-*co*-BVImCl), s-IPNs exhibited denser structures due to the entrapment of starch within the macrocavities of the copolymer structures. EDX results measured for the s-IPN/St1.0 showed a homogeneous distribution of chlorine and nitrogen atoms (from BVImCl) through the hydrogel structure.

Swelling. The water swelling capacity (WSC) of the synthesized freeze-dried hydrogels was evaluated in different media (bidistilled water, phosphate buffer (PB) and phosphate buffer saline (PBS)) at 25 °C; the swelling profiles are depicted

DOI: 10.1021/acssuschemeng.9b01071
ACS Sustainable Chem. Eng. 2019, 7, 10516−10532

in Figure 3. The WSC of the hydrogels after 24 h of immersion in different media is also presented in Figure 3D for comparison. In general terms, the WSC of the hydrogels increased in the order PBS (I = 0.169 M) < PB (I = 0.027 M) < bidistilled water (I ≈ 0 M). Water sorption equilibria (plateau in WSC profiles) were promptly attained for all the hydrogels (<1 h), which maintained their structural integrity (in all the tested media and for at least 5 months). The WSC of all polycationic hydrogels in bidistilled water (Figure 3A) was much higher than that of neutral poly(HEMA). This effect is a result of two mechanisms, namely the ionic pressure that is established between the cationic hydrogel and water (which presents negligible ionic strength) and the electrostatic repulsion between positively charged monomers present in the copolymer backbone. In the first case, water molecules diffuse into the copolymer network to dilute the higher amount of charges existing inside the hydrogel, up to a certain limit (equilibrium) that is mainly defined by the mechanical elastic response of the hydrogel. This means that the hydrogels swell, up to a certain limit which highly depends on its cross-linking degree. In the second case, electrostatic repulsion lead to an increase in the free volume in-between copolymer chains which favor water molecules to diffuse inside the hydrogel network up to a certain swelling limit as mentioned above. The effect of the ionic strength of the medium over the WSC of the hydrogels can be seen in Figures 3B-3D. The WSC of the hydrogels in saline media followed a similar trend to that observed in water (poly(HEMA) < poly(HEMA-*co*-BVImCl) < s-IPNs), however, and as expected, the presence of salts in PB and in PBS led to a significant decrease in the WSC of the cationic hydrogels (~46% in PB and 63% in PBS) when compared to WSC measured in pure water, and consequently to a lower mechanical response of the hydrogels when immersed in saline media. This result is justified by the higher ionic strengths of the saline media (0.027 M in PB and 0.169 M in PBS) when compared to water, which led to a decrease in the ionic pressure that is established between the hydrogel network and the external media (in this case both the hydrogel and the media have charges). As a consequence the amount of water that diffuses inside the hydrogel decreases because the difference between the number of charges inside and outside the hydrogel network is lower and therefore equilibrium (or charge dilution) is attained at lower WSC. Moreover the anions present in the buffer saline solutions may also induce a charge screening effect around the cationic groups of the hydrogel decreasing the electrostatic cation−cation repulsions between positively charged monomers also leading to a decrease in the ionic pressure difference between the polymer network and the external solution.[60,61] The WSC of s-IPNs were significantly higher than that of poly(HEMA-*co*-BVImCl) (× 2 and ×2.4 for s-IPN containing 0.5 and 1.0 wt % of starch, respectively) due to starch hydrophilic nature which favors hydrogel−water interactions.[62] The physicochemical and functional properties of starch depend on the raw material source (e.g., wheat, cassava, rice, maize, potato) and potato starch (that was used in this work) has one the highest water swelling capacities.[63] The WSC of starch-based s-IPNs in PBS (~360%) is significantly higher than that observed for other starch-based IPN systems, synthesized using acrylate-based monomers.[64,65]

The water vapor sorption (WVS) capacity of freeze- and oven-dried hydrogels is given in Figure 4. The equilibrium was attained in 48 h and there was no significant influence of the

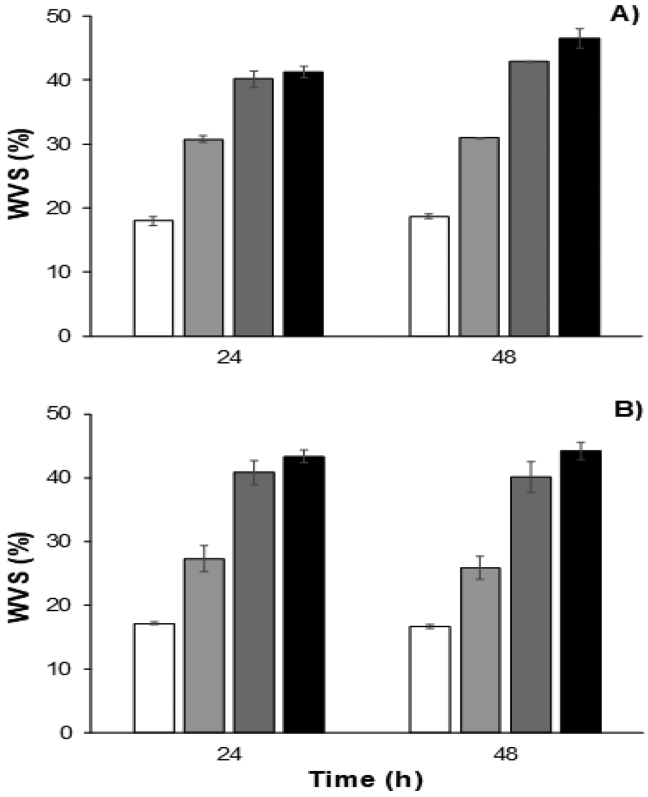

Figure 4. Water vapor sorption (WVS) capacity of the oven-dried hydrogels (A) and freeze-dried hydrogels (B) measured at RH ≥ 90% and 25 °C for poly(HEMA) (□), poly(HEMA-*co*-BVImCl) (light gray ■), s-IPN/St0.5 (medium gray ■) and s-IPN/St1.0 (■).

employed drying method on the WVS capacity of the hydrogels at 25 °C and RH ≥ 90% (no statistical difference at *p*-value >0.05). The WVS capacity of the hydrogels ranked similarly as for the WSC: poly(HEMA) < poly(HEMA-*co*-BVImCl) < s-IPN/St0.5 < s-IPN/St1.0. The WVS capacity of s-IPNs was twice that measured for poly(HEMA) which again confirms that the hydrophilic and hygroscopic character of starch and BVImCl.[66]

Interestingly, and as can be seen in Figure S2 (Supporting Information), the volume of the polycationic freeze-dried hydrogels was significantly reduced (samples shrank down to one-third their original area) after 24 h of exposure to high RH, at constant temperature revealing an effective mechanical response of these hydrogels during WVS experiments and when exposed to high RH. It is hypothesized that water vapor molecules become strongly adsorbed to the hydrogels internal pore walls, due to strong BVImCl−water and starch−water interactions, leading to condensation above a certain water vapor concentration, which ultimately lead to the collapse of the macroporous structure of the hydrogels due to hydrogen-bonding interaction among water molecules condensed within the pores.[67,68]

Thermomechanical Properties. The thermogravimetric profiles of poly(HEMA) and starch presented a one-step degradation profile (with maximum degradation peak (T_{peak}) of 385 and 306 °C, respectively) in agreement with data previously reported in the literature.[69,70] Differently, poly-(HEMA-*co*-BVImCl) and s-IPNs hydrogels presented three degradation steps with maximum T_{peak} values between 255 and 289 °C, 322−329 °C and 409−417 °C, respectively (Figure

DOI: 10.1021/acssuschemeng.9b01071
ACS Sustainable Chem. Eng. 2019, 7, 10516−10532

Table 2. Thermomechanical Data Measured for the Prepared Hydrogels[a]

Hydrogels	$Wt_{150\ °C}$ (%)[b]	$T_{5\%}$ (°C)[c]	T_{onset} (°C)[d]	T_{peak1} (°C)[e]	T_{peak2} (°C)[e]	T_{peak3} (°C)[e]	T_g (°C)[f]	G* (MPa)[g]	tan δ (−)[g]
Poly(HEMA)	2.3	332.5	349.2	–	–	385.1	117.3 ± 1.2	22.0 ± 1.2	0.14 ± 0.1
Poly(HEMA-co-BVImCl)	3.9	208.2	253.3	285.5	322.1	416.9	120.7 ± 0.9	6.4 ± 1.1	0.16 ± 0.1
s-IPN/St0.5	3.6	205.5	254.8	286.3	322.8	413.3	119.6 ± 0.2	4.9 ± 0.5	0.38 ± 0.2
s-IPN/St1.0	4.5	206.9	259.3	288.5	322.3	413.2	121.1 ± 1.8	0.6 ± 0.0	3.52 ± 0.3

[a]Parameters $Wt_{150°C}$ (%), $T_{5\%}$ (°C), T_{onset} (°C) and T_{peak} (°C) were measured by TGA; glass transition temperatures (T_g) were measured by DSC; and complex shear modulus (G*) and loss factor (tan δ) at 1 Hz were measured by rheology. [b]Weight loss (%) at 150 °C. [c]Temperature where the weight loss is 5% (wt). [d]Temperature at which thermal degradation starts to occur. [e]Maximum degradation temperature from DTG curves (obtained from first derivative of weight loss vs temperature curve). [f]Obtained from the integration of a "step" of heat flow vs temperature curve. [g]According to literature.[52]

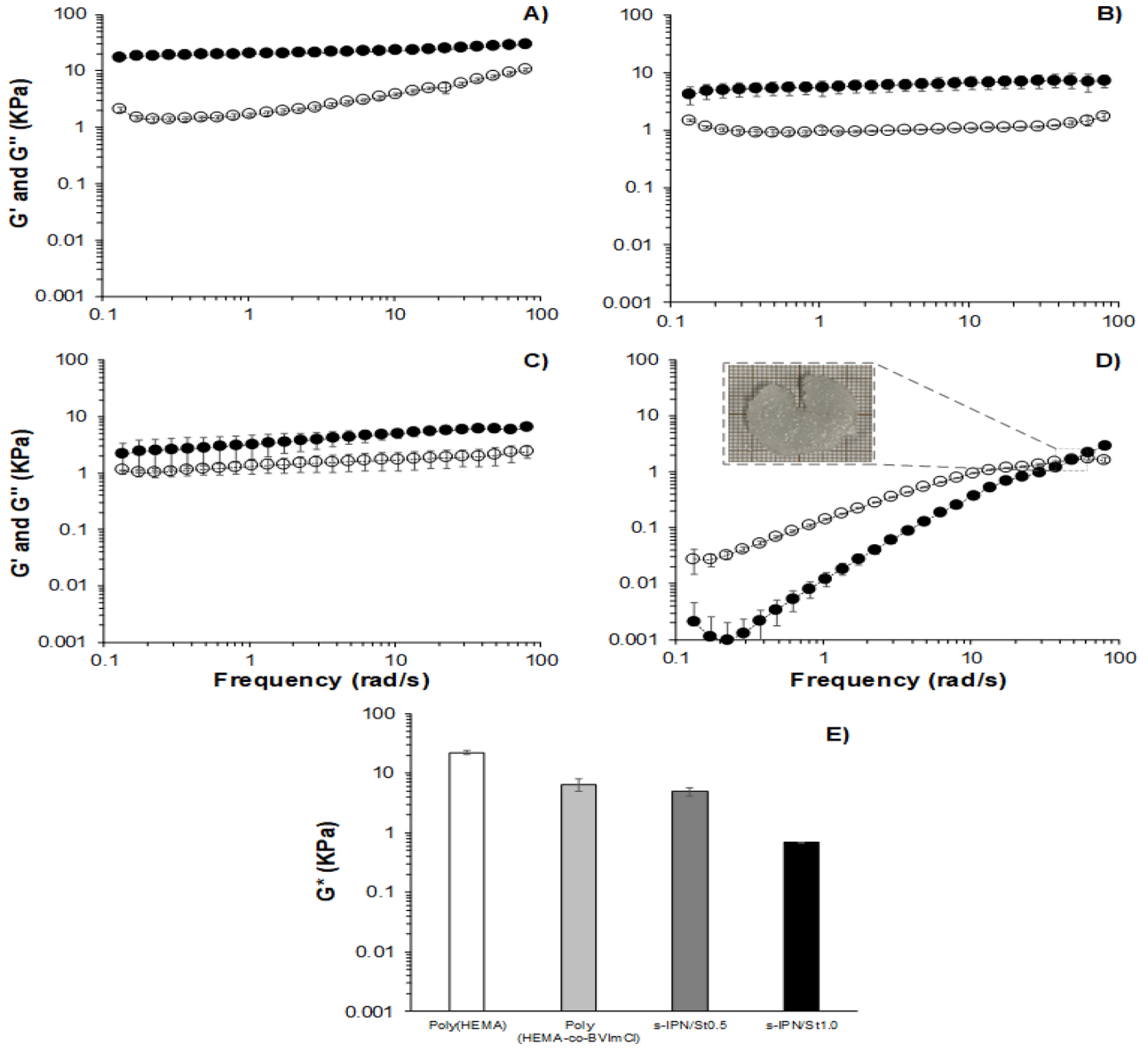

Figure 5. Rheological measurements of hydrogels hydrated in bidistilled water at 25 °C (at equilibrium): (A) Poly(HEMA), (B) Poly(HEMA-co-BVImCl), (C) s-IPN/St0.5, (D) s-IPN/St1.0. The viscoelastic properties are represented as shear/storage modulus (G', λ), loss modulus (G'', ■), and loss factor (tan δ, ν) as a function of oscillatory frequency. (E) Complex shear modulus (G^*) calculated for a frequency of 1 Hz.

S3, Supporting Information and Table 2). These events may result from the thermal degradation of BVImCl, HEMA-*co*-BVImCl and HEMA rich domains, respectively that may be present along the polycationic structure. Moreover, TGA results also indicated that the thermal stabilities of the polycationic hydrogels are similar and lower than that of the neat poly(HEMA) (Table 2). Polycationic hydrogels also present higher weight losses at ∼150 °C (up to 4.5 wt %), which can be attributed to residual water evaporation and which confirms that the presence of the IL increased the hydrophilicity of the hydrogels (when compared to poly(HEMA)).

DOI: 10.1021/acssuschemeng.9b01071
ACS Sustainable Chem. Eng. 2019, 7, 10516−10532

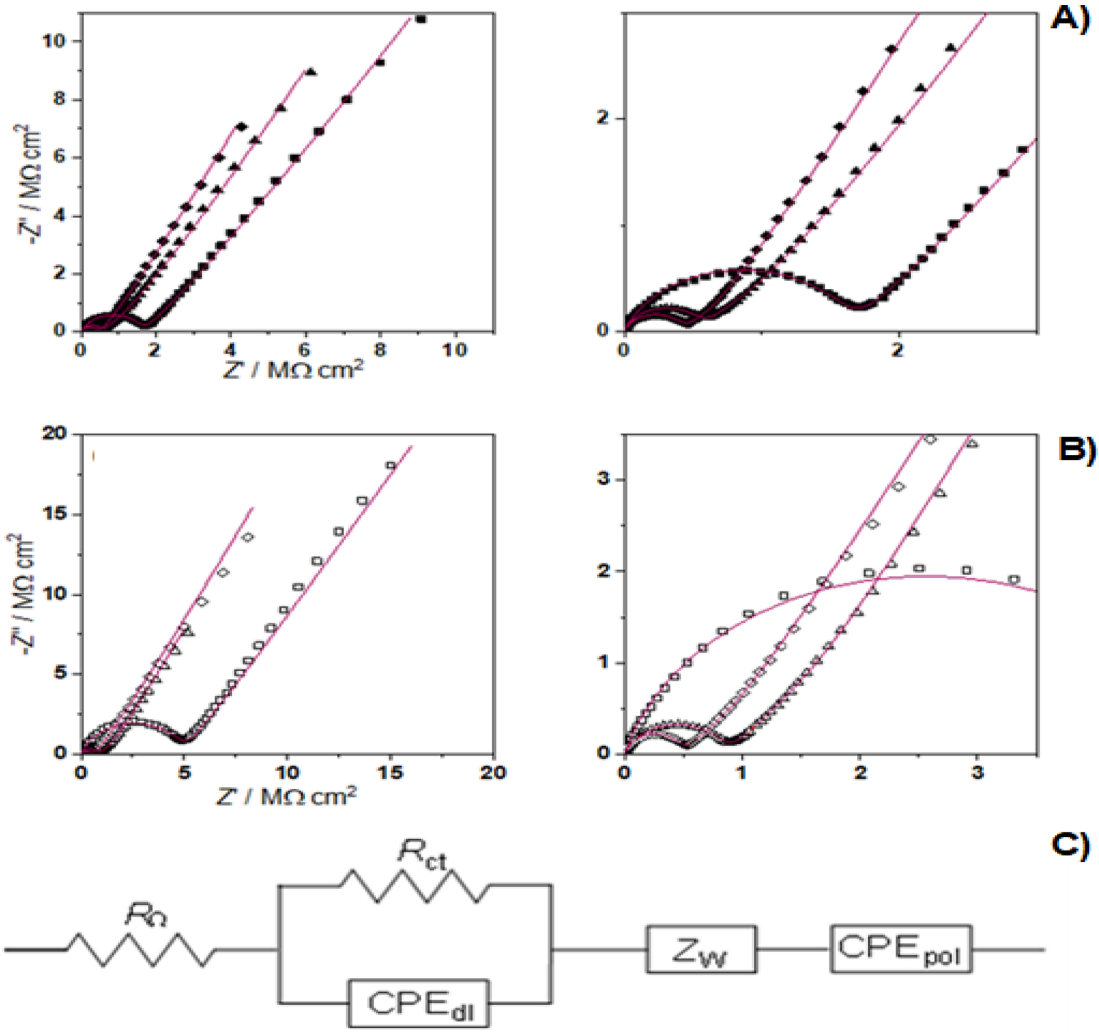

Figure 6. Complex plane plots obtained for prepared hydrogels: poly(HEMA-co-BVImCl) (■, □), s-IPN/St0.5 (▲, Δ) and s-IPN/St1.0 (♦, ◊) where filled and open symbols represent freeze-dried (A) and oven-dried (B) hydrogels, respectively. The equivalent circuit used to fit the impedance spectra is represented in Figure 6C.

The effect of IL-functionalization over poly(HEMA) chain mobility was indirectly accessed by comparing the glass transition temperatures (T_g) of the prepared hydrogels (determined from DSC analysis). The T_g of the poly(HEMA) homopolymer measured was determined as 117.3 ± 1.2 °C (Table 2 and Figure S3, Supporting Information) which is in reasonable agreement with the value of ∼115 °C previously reported in the literature.[71] The T_g value measured for s-IPN/St1.0 (121.1 ± 1.8 °C) is also in agreement with that previously reported for poly(HEMA)-starch composites, (∼120 °C).[72] No statistically significant difference (p-value >0.05) was observed for T_g values of poly(HEMA) and of polycationic samples (poly(HEMA-co-BVImCl) and s-IPNs), which indicates that the thermomechanical properties of poly(HEMA) are mostly maintained after functionalization, probably due to the relative low amount of IL incorporated in the copolymer backbone.

The viscoelastic properties of water-swollen hydrogels (at equilibrium) were measured by oscillatory frequency sweeps at 25 °C, and the results are presented as the change of the storage modulus (G') and of the loss modulus (G'') as a function of the angular frequency of tested hydrogels (Figure 5A). The complex shear modulus (G^*) was calculated from G' and G'' data and as previously described in the literature,[50] and the results are presented in Table 2 and Figure 5B. With the exception of s-IPN/St1.0, all hydrogels presented a typical frequency dependent gel-like behavior ($G' > G''$ and tan $\delta < 1$, over the frequency range analyzed), converging to a plateau (Figure 5A). A similar gel-like behavior was previously reported for poly(HEMA) hydrogels cross-linked with diethylene glycol dimethacrylate at 25 °C.[73] For the frequency range analyzed, G', G'' and G^* values measured for poly(HEMA-co-BVImCl) and s-IPN samples were lower (up to 10× lower) than those measured for poly(HEMA) according to the sequence poly(HEMA) > poly(HEMA-co-BVImCl) > s-IPN/St0.5 > s-IPN/St1.0, meaning that poly(HEMA-co-BVImCl) and s-IPN samples present a lower capacity to store mechanical perturbation in the form of elastic deformation (Table 2). This sequence follows the inverse trend observed for the water swelling capacity of the samples (Figure 3). Therefore, these results indicate that the water content of the hydrogels plays a major role in their viscoelastic properties[74] by enhancing hydrogel chain mobility (by disrupting interchain hydrogen bonding), thus softening its network and increasing its flexibility. The rheological properties of s-IPN/St1.0 were strongly dependent on the applied

DOI: 10.1021/acssuschemeng.9b01071
ACS Sustainable Chem. Eng. 2019, 7, 10516−10532

Table 3. Equivalent Circuit Element Values Obtained from Fitting EIS Spectra Shown in Figure 6, for Oven-Dried and for Freeze-Dried Hydrogels

Hydrogels	R_{ct} (kΩ cm^2)	CPE_{dl} (pF s$^{\alpha-1}$ cm^{-2})	a_1	^aZ_w (kΩ s$^{\alpha-1}$ cm^2)	$^a\rho$ (MΩ cm)	$^a\sigma$ (S cm^{-1})	τ (ms)	a_w	$^aCPE_{pol}$ (nF s$^{\alpha-1}$ cm^{-1})	a_2
Oven-dried hydrogels										
Poly(HEMA-co-BVImCl)	4870	140	0.83	1230	16.4	0.1	760	0.5	3.1	0.66
s-IPN/St0.5	841	132	0.8	1350	22.5	0.2	300	0.41	7	0.68
s-IPN/St1.0	471	41	0.92	595	7.4	2	41	0.42	6.6	0.62
Freeze-dried hydrogels										
Poly(HEMA-co-BVImCl)	1650	192	0.77	163	1.6	0.7	142	0.48	11.4	0.59
s-IPN/St0.5	530	135	0.84	480	4	3.2	38	0.41	15.8	0.6
s-IPN/St1.0	413	188	0.81	345	2.5	5.2	27	0.4	28.6	0.59

[a]Values normalized by sample thickness.

frequency, presenting a viscous-like behavior ($G' < G''$ and tan $\delta > 1$) at frequencies below 50 rad/s and a crossover point at ~50 rad/s, which resulted from an overload of the applied mechanical perturbation over the intermolecular forces of the s-IPN/St1.0 structure that led to the rupture of the hydrogel (image in Figure 5A).

Finally, and as can be observed in Table 2, the tan δ value measured for poly(HEMA-co-BVImCl) was similar to that of poly(HEMA) while higher tan δ values were obtained for s-IPN samples, and they increased with the amount of starch in the s-IPN structure. Higher loss factors (tan $\delta > 0.1$) are typical of biological gels and soft tissues.[75]

Electrochemical Properties. The effect of IL and starch contents on the electrical resistivity of prepared polycationic hydrogels was evaluated by electrochemical impedance spectroscopy. A symmetrical cell with two steel electrodes was used and hydrogels were placed in between the two electrodes. Additionally, the effect of hydrogel porosity on its electrical resistivity was also assessed by analyzing both dense and porous samples which were obtained by conventional drying (in an oven at 50 °C) and by freeze-drying, respectively. Since the electrical resistivity of hydrogels is greatly affected by their water contents,[76] all samples were maintained in controlled relative humidity (RH ≥ 90%), at 25 °C, and overnight before analysis. The impedance spectra of the polycationic hydrogels are shown in Figure 6A,B, for freeze-dried and oven-dried samples, respectively. The spectrum of poly(HEMA) is not represented due to the high resistivity of this sample, which behaves as an insulator under the employed conditions. Therefore, and as a first conclusion, these results show that IL-functionalization induces an increase in the electrical conductivity of the poly(HEMA)-based hydrogels. As can be seen in Figure 6A,B, all spectra presented a semicircle at higher to intermediate frequencies (due to charge transfer reactions, and to a nonideal double layer capacitance at the film/electrode interface), diffusive lines at intermediate/low frequencies (due to ion diffusion through the hydrogel), followed by capacitive lines at lower frequencies (due to charge separation processes in the bulk of the hydrogel). The values of the resistive and capacitive elements were estimated by fitting the impedance spectra to the equivalent circuit model (Figure 6C), and the results are presented in Table 3. According to the equivalent circuit model (Figure 6C), all fitted spectra present a cell resistance (R_Ω) that comprises the resistance intrinsic to the equipment (electrical contacts, wires and steel electrodes). The obtained value of R_Ω (5.0 ± 2.8 kΩ) is not presented in Table 3 since the cell resistance R_Ω is not related to the sample electrical characteristics. The equivalent circuit is further described by a parallel combination of a charge-transfer resistance (R_{ct}) with a nonideal double layer capacitance (CPE_{dl}), in series with a Warburg diffusional resistance (Z_w), followed by a polarization capacitance (CPE_{pol}).

As observed, when comparing the equivalent circuit values from Table 3 for oven- and freeze-dried polycationic hydrogels (poly(HEMA-co-BVImCl) and s-IPNs), it can be seen that freeze-drying leads to a decrease in R_{ct} and Z_w values, and to an increase in the CPE_{pol} values. This confirms that the morphology of the hydrogels has a major influence on the ion conductivity through their physical structure. Since the drying process influences hydrogels porosity, the freeze-dried samples are more porous and therefore less resistive when compared to the oven-dried ones. Porous structures enhance the diffusivity of ions through the swollen network channels (working as "shortcuts") and resulting in higher conductivity,[77,78] although being also dependent on geometric properties such as pore interconnectivity, size, shape and tortuosity.[78−80]

Nevertheless, data presented in Table 3 show that the amount of starch significantly influences all the equivalent circuit elements: the increase in starch content led to a decrease in the R_{ct} and Z_w values, and to an increase in the CPE_{pol} values. The ionic conductivities of freeze-dried hydrogels increase according to the sequence poly(HEMA-co-BVImCl) < s-IPN/St0.5 < s-IPN/St1.0, which may be explained in terms of the water vapor content of each hydrogel, which increases with the amount of starch (Figure 4). Higher water contents are known to enhance free chloride anions diffusivity through the hydrogel network, and consequently to increase the ionic conductivity of polyelectrolyte-based materials.[76]

Recent studies on the electrochemical properties of several materials functionalized with different ionic liquids have reported ionic conductivities ranging between 10^{-6} and 10^{-2} S cm^{-1} at room temperature (~25 °C).[29,30,77,81,82] The ionic conductivity values obtained in the present work for prepared polycationic hydrogels were significantly higher than those reported so far, which is most probably due to the high water contents (>40 wt %) of these samples and to the homogeneous distribution of BVImCl through the hydrogel network that was achieved in these samples (as confirmed by SEM-EDX). Nevertheless, it is important to refer that conductivity measurements of IL-functionalized materials are very much dependent on a large number of variables, including the chemical composition and morphology of the studied material (IL types and compositions, charge densities and charge

DOI: 10.1021/acssuschemeng.9b01071
ACS Sustainable Chem. Eng. 2019, 7, 10516−10532

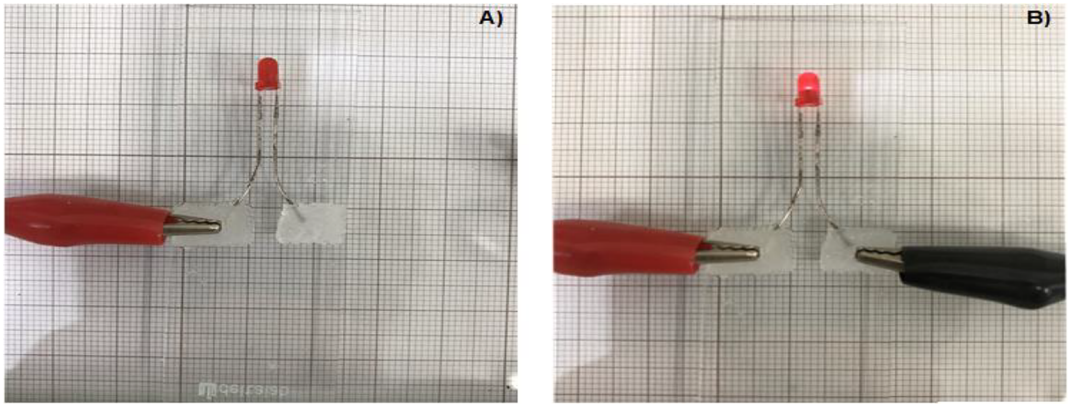

Figure 7. Schematic representation of electronic conductivity response of s-IPN/St1.0 hydrogel (in water equilibrium) before (A) and after (B) the application of a potential difference of 1 V at room temperature (~25 °C).

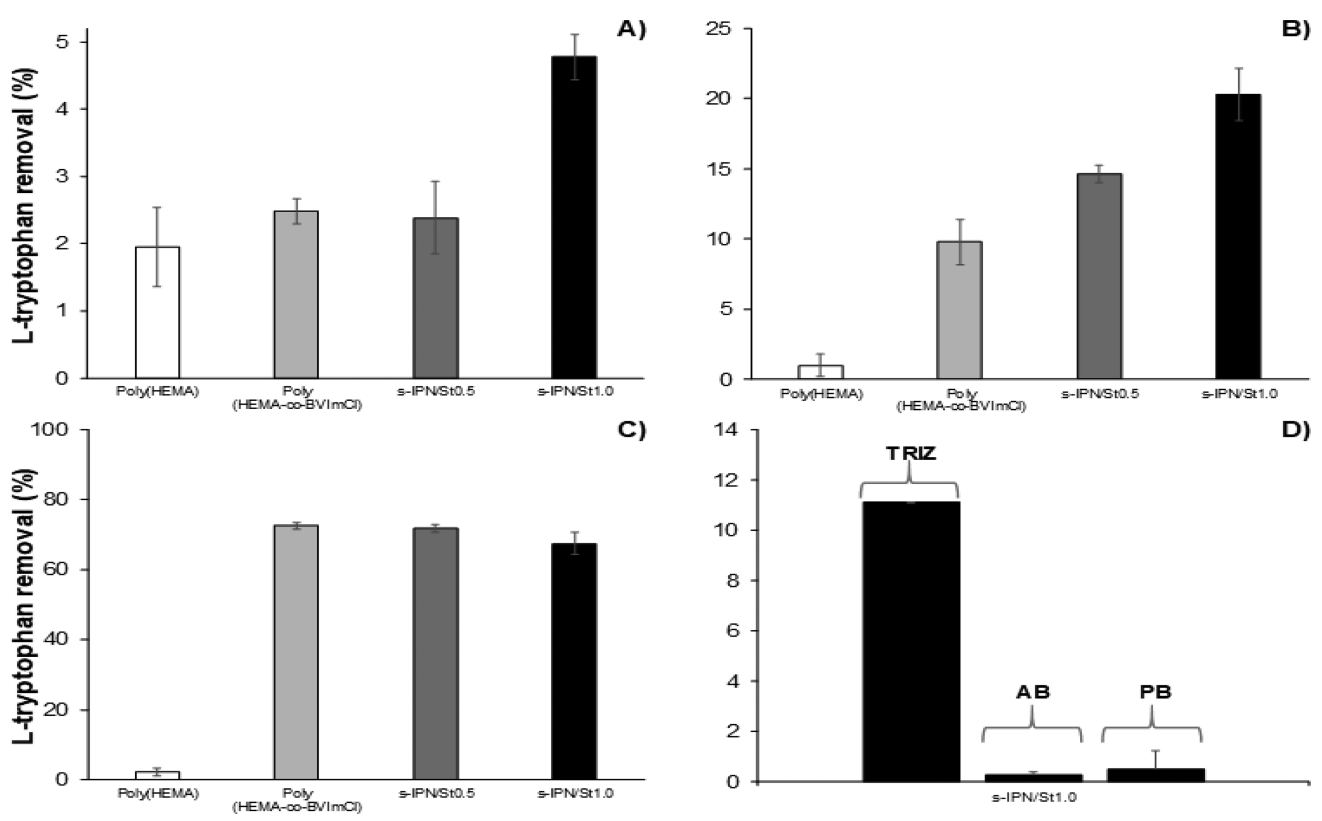

Figure 8. Electro-assisted sorption of L-tryptophan [50.3 mg/L] in bidistilled water at 0 V (A), 2 V (B), and 100 V (C) and in different aqueous media: Trizma base buffer (TRIZ), acetate buffer (AB), and phosphate buffer (PB) at 2 V (D) at room temperature (~25 °C).

distributions, presence of spacers, purities, etc.), as well as on the experimental measuring conditions (setup, temperature, relative humidity, etc.) which clearly hamper fair/clear comparisons between different works.

Finally, another interesting feature of the prepared cationic hydrogels is that they both present ionic and electronic conductivities. As illustrated in Figure 7, s-IPN/St1.0 mediates electron transfer onto a LED under a DC current of 1 V at room temperature (~25 °C). It is hypothesized that this hydrogel behaves as a single-ion conducting material where the transport of electrons, and consequently the electrical conductivity, resulted from oxidation of Cl^- ions at the anode. This allows the generation of small electrical currents (269 μA, measured with a multimeter) through the hydrogel, which reveals some potential for the application of these materials as electrochemical devices such as fuel cells, batteries, etc.

Electro-Assisted Sorption/Desorption of L-Tryptophan. The sorption/desorption capacity of the prepared polycationic hydrogels toward L-tryptophan (Try) (used as a model charged biomolecule) was evaluated for samples immersed in different aqueous media and submitted to different applied electrical stimuli. The capacity to control the removal/release of charged biomolecules from aqueous media is advantageous to optimize (bio)separation processes and for the development of controlled release devices in general and for potential Try-based therapeutic applications in particular (such as anxiety and depression).[83]

Electro-assisted sorption (at an applied voltage of 2 and 100 V) and desorption (at an applied voltage of 2 and 5 V)

DOI: 10.1021/acssuschemeng.9b01071
ACS Sustainable Chem. Eng. 2019, 7, 10516−10532

experiments were carried out at room temperature (~25 °C), and the results are presented in Figure 8 and Figure 9,

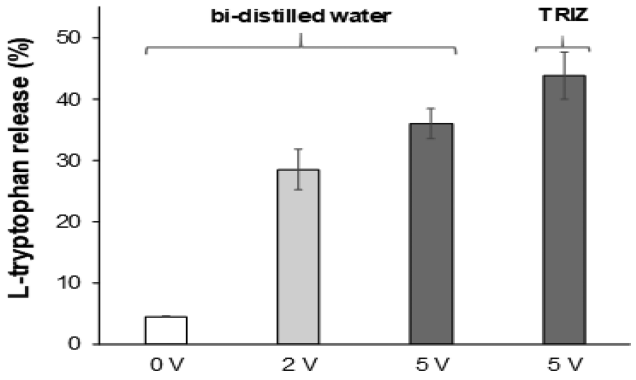

Figure 9. Electro-assisted desorption of L-tryptophan [50.3 mg/L] for s-IPN/St1.0 in different media, namely bidistilled water and Trizma base buffer (TRIZ), at different applied voltages (0, 2, and 5 V) at room temperature (~25 °C). The distance between the electrodes was 3 cm, and the experiments were carried out in a constant volume (18 mL) of amino acid solution.

respectively. Conventional sorption/desorption experiments (passive sorption with no applied voltage) were also performed for comparison purposes. The total number of moles of Try in solution (4.4 μmol, in 18 mL of a solution with a concentration of 50.3 mg/L) was confirmed to be lower than the estimated number of moles of ionic liquid (~21.4 μmol) present in ~20 mg of the s-IPN/St1.0 hydrogel (as calculated from data given in Table 1).

As can be seen in Figure 8A, when no electrical potential is applied, the amino acid sorption capacity of the hydrogels, poly(HEMA-co-BVImCl), and s-IPN/St0.5 was similar (p-value >0.05) to that of poly(HEMA) while the sorption capacity of s-IPN/St1.0 is almost twice the values of the other hydrogels. This indicates that, under these experimental conditions (25 °C and 0 V), the Try sorption capacity of poly(HEMA-co-BVImCl) and s-IPN/St0.5 is mainly governed by amino acid diffusion into the hydrogel matrix rather than by IL–amino acid electrostatic interactions (since the water sorption capacity was found to be more dependent on hydrogels WSC than on their IL content). The higher passive-sorption capacity observed for s-IPN/St1.0 may result from the slightly higher IL content in this sample (Table 1) which may promote enhanced hydrogel/Try electrostatic interactions, and higher WSC (Figure 3), which will improve Try diffusion into the hydrogel matrix.

The effect of an applied voltage on Try sorption capacity is presented in Figure 8Band8C, for samples submitted to DC voltages of 2 and 100 V, respectively. Results show that the Try sorption capacity was significantly improved, compared to passive sorption, even at the lowest applied potential. Moreover, it was interesting to notice that at the lowest applied voltage (Figure 8B) it is possible to modulate the Try sorption capacity of the hydrogels.

During the electro-assisted sorption experiments of polycationic hydrogels (poly(HEMA-co-BVImCl) and s-IPNs), it was observed that the pH of the employed media decreased to ~4.5. This happens because when the electrical stimulus is applied, free chloride anions (from BVimCl) move toward the positively charged electrode (anode), while positively charged imidazolium cations cannot move (to the cathode) since they are covalently attached to the hydrogel network. At the anode, oxidative reactions take place leading to the formation of hydrochloric and hypochlorous acids in aqueous media[84] which justifies the observed decrease in the pH of the amino acid solution. Notice that at a pH of 4.5, the concentration of positively charged amino acid molecules ([NH_3^+–R–COOH]) increases, since this pH is lower than the isoelectric point of L-tryptophan, which is equal to 5.89[85,86] and therefore, electrostatic interactions between Try and the polycationic hydrogels are not favored. Nevertheless, the electro-assisted sorption increased up to 20% at 2 V and up to 70% at 100 V, when compared to results obtained from passive sorption (0 V). The average amount of Try absorbed/adsorbed by passive sorption after 10 days was 14.6 ± 6.1% which is lower than that obtained by electro-assisted sorption at 2 V for s-IPN/St1.0, and for all polycationic hydrogels at 100 V, only after 3 h. When an electrical potential is applied, the concentration of positively charged Try species ([NH_3^+–R–COOH]) increases in the vicinity of the anode, while the concentration of negatively charged species ([NH_2–R–COO^-]) increases at the cathode as a result of water hydrolysis, which induces the formation of hydronium ions (acidic pH) at the anode and hydroxide ions (alkaline pH) at the cathode. As their concentration increases, protonated species are attracted to the cathode while deprotonated species are attracted to the anode. This migration between electrodes, induced by the applied voltage, promotes interactions between [NH_2–R–COO^-] and the polycationic hydrogel and consequently its adsorption from the medium. Such an effect was more evident at higher applied potential (100 V, Figure 8C) because the driving force that enhances charged Try diffusion increases, leading to higher Try sorption capacity (>65% compared to poly(HEMA)).[87] Moreover, no significant difference (p-value > 0.05) was observed for the sorption capacity of all tested polycationic hydrogels at 100 V suggesting that the total amount of Try absorbed/adsorbed was mainly governed by the amount of cationic functional groups available to establish electrostatic interactions in each hydrogel, which are similar for all samples (Table 1).

It is important to refer that, during the experiments performed at 100 V, a brownish foam was formed near both electrodes probably resulting from the hypochlorous acid-mediated oxidation of Try molecules.[88] The amount of Try oxidized in the electrodes was quantified (after careful removal of the foam adhered to the electrodes) leading to ~4.4 ± 0.17% of the initial amount of Try in solution. The side of hydrogel facing the cathode also showed a brown-colored layer; however, the bulk solution did not present any evidence of Try oxidation, and as was confirmed by the comparison of the UV spectra of the Try solution before and after the electro-assisted experiment (at 100 V for 3 h) (Figure S4, Supporting Information). Overall, these findings indicate that it is possible to modulate Try, or even other amino acid, removal from aqueous media by controlling the intensity of the applied DC current. Moreover, and although the electro-sorption experiments carried out at 100 V led to some degree of oxidation of Try, these results indicate potential applications of these cationic hydrogels in processes for which the integrity of the molecules is not a relevant requisite (e.g., wastewater treatment, (bio)remediation), or for the removal/separation of molecules less sensitive to degradation under electrical potential stimulus.

DOI: 10.1021/acssuschemeng.9b01071
ACS Sustainable Chem. Eng. 2019, 7, 10516–10532

The effect of the nature of the medium and of pH on the electro-assisted sorption was also evaluated for s-IPN/St1.0 hydrogels, since they presented the highest electro-assisted Try sorption yield in water (Figure 8D). The quantification of Try removed/release in bidistilled water, and in TRIZ and AB buffers, was performed according to previously constructed calibration curves at 25 °C. The spectra of Try after electro-assisted desorption experiments at 5 V was confirmed by UV spectrophotometry (Figure S4, Supporting Information). Preliminary electro-assisted sorption experiments were also performed in PBS buffer, however the oxidation of Try was evident even at lower applied voltage.

The Try sorption capacity of the hydrogels immersed in Trizma base buffer, used to avoid pH changes during the experiments, decreased to ~11.1 ± 0.02%. During these experiments, only a slight decrease of pH was observed from 9.9 to 9.3, indicating that Try molecules were mostly negatively charged ($[NH_2-R-COO^-]$). These results suggest that the hydrogel sorption capacity depends on the electrophoretic flow of Try charged molecules between electrodes. When an electrical potential is applied in the Trizma base buffer medium, a unidirectional migration of negatively charged Try molecules is stablished from the cathode to anode, restraining ionic interactions with the s-IPN/St1.0 hydrogel.

Negligible Try removal (≤0.1%) was observed for hydrogels immersed in acidic and neutral buffer media as shown in Figure 8D. At low pH (below the isoelectric point of L-tryptophan), ionic interactions between positively charged Try species and the polycationic hydrogel are not favored. When s-IPN/St1.0 samples were immersed in the neutral phosphate buffer medium, significant gel shrinkage was observed what may have hampered Try diffusion into the hydrogel network and further interactions with the cationic hydrogel. Gel shrinkage was hypothesized to be due to the divalent phosphate anions (HPO_4^{2-}) present in the buffer that may have worked as ionic cross-linkers of the polycationic hydrogel chains, thus decreasing the number of cationic groups that were available to adsorb Try. This behavior was not observed in any of the other tested monovalent-based aqueous solutions. Moreover, when hydrogels previously soaked in the phosphate buffer were immersed in bidistilled water at room temperature, they remained shrunken confirming the presence of relatively strong ionic cross-linking.

Desorption/release experiments of Try from the hydrogel s-IPN/St1.0 were carried out at low applied voltages (0, 2, and 5 V), to avoid Try oxidation, with samples previously exposed to the same sorption conditions (at 25 °C and 2 V, for 3 h in bidistilled water). The results presented in Figure 9show that Try desorption into water under an applied voltage of 2 V is 24% higher than for passive desorption (0 V). The delivery of charged species from an electrically responsive hydrogel may depend on three main mechanisms namely, electrically induced swelling/deswelling (which alters pore sizes leading to different diffusion kinetics), electrically induced erosion of hydrogel (release of charged species due to network degradation), and electrophoresis (migration of charged molecules through the hydrogel induced by an electrical field).[89] In this work, since no induced swelling/deswelling and/or erosion of the hydrogel s-IPN/St1.0 was observed during electro-assisted experiments, it was assumed that Try desorption/release occurs mainly by electrophoresis, and considering that passive desorption is governed only by Try diffusion from the hydrogel to the medium due to gradient concentrations. A further increase in the applied potential (5 V) led to an increase in the amount of amino acid released to the medium (~7.5%) when compared to results obtained at 2 V. Recent studies on the effect of the applied electrical stimulus on the release of acetyl salicylic acid from a polysaccharide-based hydrogel also showed an increase of ~30% after an increase of the applied electrical stimulus from 0 up to 5 V.[90]

The electro-assisted desorption of L-tryptophan into TRIZ was also carried out at 5 V. Figure 9 shows that the release of Try was higher in TRIZ (~7.8%) than in bidistilled water, during 3 h of measurements at 5 V. This might be explained in terms of the different amounts of amino acid that were previously adsorbed in each sample. It was expected that, for a lower quantity of adsorbed amino acid, a higher desorption percentage would be obtained during 3 h of measurements. However, and due to the fact that the amount of adsorbed amino acid in bidistilled water and TRIZ differ significantly, it is not possible to perform a direct comparison between the amounts of L-tryptophan desorbed in these two situations. Any evidence of Try degradation was observed as confirmed from the UV spectra of Try molecules after electro-assisted desorption/release experiments at 2 and 5 V (Figure S4, Supporting Information).

Different IL-based liquid–liquid extraction systems were previously tested for the separation of Try from aqueous media.[91−93] The highest Try removal capacity (96%) reported in those works was observed when using the water/potassium phosphate/1-butyl-3-methylimidazolium methylsulfonate ABS system, after 24 h of contact.[91] To the best of our knowledge, there are no previous studies on the separation/removal of Try from aqueous environments using electro-responsive hydrogels based on ILs. Therefore, this work presents innovative research on the development of IL-based materials for the controlled and selective removal/separation and/or release of biomolecules, depending on the charge of the target molecule, on the chemical composition of the hydrogels, on the medium and on the applied electric stimulus.

Cytocompatibility. The cytocompatibility of the freeze-dried hydrogels was evaluated for Balb/3T3 fibroblasts by cell viability (LDH) and the cell proliferation (MTT) assays (Figure 10A,B). As can be seen in Figure 10A, and after 48 h of direct contact, LDH results clearly showed high cell viabilities (~100%) for all hydrogels, meaning that tested samples did not induce cell wall lysis. It has been reported that the toxicity of ILs depends on not only many structural variables such as cation/anion alkyl chain length, cation/anion type, presence of specific functional groups but also external factors such as the nature of the cell line tested.[22,94] For example, ILs bearing short alkyl chain lengths (number of carbons lower than six), and chloride counterions, tend to be less toxic.[95,96] Moreover, the polymerization of IL-based monomers is known to decrease further their cytotoxicities.[97] However, and as can be seen in Figure 10B, the presence of the IL in the poly(HEMA-co-BVImCl) hydrogel seems to affect fibroblast metabolic activity, mostly if compared with poly(HEMA) (which is well-known for its relative good biocompatibility).[98] In a previous study, the cytotoxicity of several imidazolium-based ionic liquids against normal fetal lung fibroblasts by using the MTT assay was also reported. In particular, 1-butyl-3-methylimidazolium salicylate presented high cytotoxicity, even at low concentrations, and when compared to other imidazolium-based ionic liquids containing the same anion but longer alkyl chains.[99] These results seem to indicate that the

DOI: 10.1021/acssuschemeng.9b01071
ACS Sustainable Chem. Eng. 2019, 7, 10516−10532

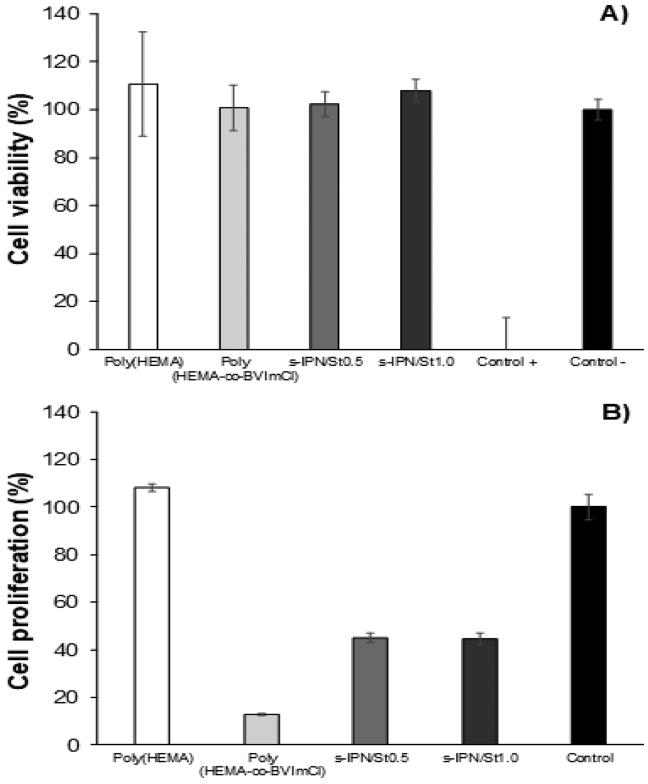

Figure 10. In vitro cytocompatibility of the prepared hydrogels tested against fibroblasts measured by the cell viability, LDH (A) and the cell proliferation, MTT (B) assays.

mechanism by which ILs affect cell metabolic activity, as measured by the MTT assay, does not depend only on the IL alkyl chain. The cationic nature of vinylpyridinium-based PILs has been previously reported as the main responsible for cell growth inhibition (against mouse fibroblasts and hamster ovary cells) due to electrostatic complexation of the polycation with negatively charged biomolecules present in cell membranes (such as proteins or phospholipids).[100] However, the capacity to inhibit cell proliferation, as observed for poly(HEMA-co-BVImCl), is interesting for other applications such as the development of antifouling materials, thus avoiding materials biodegradation and consequent loss of function during usage in aqueous media.

An increase of 30% in cell proliferation was observed for the prepared s-IPNs, independently of the employed starch composition (p-value > 0.05), when compared to poly(HEMA-co-BVImCl) samples (Figure 10B). This result can be explained by the natural biocompatibility of starch[46,47,101] which may have balanced poly(HEMA-co-BVImCl) inherent cytotoxicity. Previous studies on the influence of starch concentration over cell viability of chitosan-starch microparticles (measured by MTS assay against osteoblast cell line Saos-2) showed a significant increase of 20% in cell viability with starch concentration, which is in agreement with data herein reported.[102] Therefore, and contrary to poly(HEMA-co-BVImCl), s-IPNs have the potential to be further optimized for the development of biomaterials with improved biocompatibility and biodegradability envisaged for biomedical/pharmaceutical applications such as controlled drug delivery devices and/or scaffolds for tissue engineering.

CONCLUSIONS

This work evidenced the potential of semi-interpenetrating polymer networks (s-IPNs) as an efficient strategy to develop multi-stimuli-responsive IL-based cationic hydrogels for the electro-assisted removal/separation/release of charged molecules. The employed strategy makes use of starch, as a biocompatible, biodegradable, and low cost biopolymer obtained from renewable sources, to tune the physicochemical, rheological, electrical, and biological properties of IL-based copolymers. Another major feature of this approach is that it uses relatively low IL amounts and originates hydrogels presenting long-term stability and functionality in aqueous media, thus avoiding IL loss/contamination during usage.

The obtained hydrogels were responsive to changes in relative humidity, ionic strength, and electrical current. Compared to the copolymer poly(HEMA-*co*-BVImCl), freeze-dried s-IPNs exhibited higher water sorption capacity, ionic/electrical conductivity (5.2 S cm^{-1}), fibroblast proliferation capacity, and loss factors which are typical of biological gels and soft tissues. These materials can find applications in electro-membrane extraction processes (e.g., bioseparation processes, wastewater treatment processes, (bio)remediation, etc). In this work the electro-assisted sorption/release capacity of L-tryptophan from the prepared hydrogels was studied as a proof of concept. Results showed that the sorption/release capacity of this charged molecule can be easily tuned by modifying the intensity of the applied potential, the medium and the chemical composition of the hydrogel. It can be theorized that sorption/desorption of L-tryptophan resulted from a combined mechanism of electrophoretic flow and electrostatic interactions of the L-tryptophan with the cationic hydrogel. Moreover, and considering that the controlled sorption/release of molecules by/from electro-responsive systems depends on a large number of other variables including duration of the electrical stimulus, intrinsic properties of the electro-responsive material (degree of cross-linking and swelling/deswelling/shrinking behavior), and relative position of the samples and electrodes it is possible to assume that the systems developed in this work can be further optimized.

ASSOCIATED CONTENT

Supporting Information

The Supporting Information is available free of charge on the ACS Publications website at DOI: 10.1021/acssuschemeng.9b01071.

SEM micrographs of the cross sections of freeze-dried hydrogels and elemental mapping of nitrogen and chlorine distribution through the hydrogel s-IPN/St1.0, analyzed by EDX; mechanical response of oven- and freeze-dried hydrogels during WVS measurements at RH ≥ 90% and 25 °C; thermogravimetric profiles and DSC thermograms of the prepared hydrogels; UV−visible spectra of L-tryptophan solutions in different media after electro-assisted sorption experiments; elemental analysis results (PDF)

AUTHOR INFORMATION

Corresponding Authors

*A. M. A. Dias. E-mail: adias@eq uc.pt.
*H. C. de Sousa. E-mail: hsousa@eq uc.pt.

DOI: 10.1021/acssuschemeng.9b01071
ACS Sustainable Chem. Eng. 2019, 7, 10516−10532

ORCID

Christopher M. A. Brett: 0000-0002-1972-4434
Carmen Alvarez-Lorenzo: 0000-0002-8546-7085
Angel Concheiro: 0000-0003-0507-049X
Hermínio C. de Sousa: 0000-0002-2629-7805
Ana M. A. Dias: 0000-0002-0865-0257

Notes

The authors declare no competing financial interest.

■ ACKNOWLEDGMENTS

This work was financially supported by Fundação para a Ciência e Tecnologia (FCT-MEC) Portugal under contract UID/EQU/00102/2013, and MINECO (SAF2017-83118-R) Spain, Agencia Estatal de Investigación (AEI) Spain, and FEDER. A. M. A. Dias acknowledges FCT-MEC for a contract under the program Investigador FCT IF/00455/2013. A. Kanaan acknowledges CNPq, Brazil, for the scholarship with reference 200808/2014-1. Authors also acknowledge Dr. Fernando Augusto Pinto Garcia for providing the electrophoresis power supply EPS 500/400 (Pharmacia Fine Chemicals, Sweden).

■ REFERENCES

(1) Ferreira, N. N.; Ferreira, L. M. B.; Cardoso, V. M. O.; Boni, F. I.; Souza, A. L. R.; Gremião, M. P. D. Recent advances in smart hydrogels for biomedical applications: From self-assembly to functional properties. *Eur. Polym. J.* **2018**, *99*, 117−133.
(2) Mahinroosta, M.; Farsangi, Z. J.; Allahverdi, A.; Shakoori, Z. Hydrogels as intelligent materials: A brief review of synthesis, properties and applications. *Mater. Today Chem.* **2018**, *8*, 42−55.
(3) Ferreira, N. N.; Ferreira, L. M. B.; Cardoso, V. M. O.; Boni, F. I.; Souza, A. L. R.; Gremião, M. P. D. Recent advances in smart hydrogels for biomedical applications: From self-assembly to functional approaches. *Eur. Polym. J.* **2018**, *99*, 117−133.
(4) Li, X.; Su, X. Multifunctional smart hydrogels: potential in tissue engineering and cancer therapy. *J. Mater. Chem. B* **2018**, *6*, 4714−4730.
(5) Adesanya, K.; Vanderleyden, E.; Embrechts, A.; Glazer, P.; Mendes, E.; Dubruel, P. Properties of electrically responsive hydrogels as a potential dynamic tool for biomedical applications. *J. Appl. Polym. Sci.* **2014**, *131*, 1−9.
(6) Pairatwachapun, S.; Paradee, N.; Sirivat, A. Controlled release of acetylsalicylic acid from polythiophene/carrageenan hydrogel via electrical stimulation. *Carbohydr. Polym.* **2016**, *137*, 214−221.
(7) Yuk, H.; Lu, B.; Zhao, X. Hydrogel bioelectronics. *Chem. Soc. Rev.* **2019**, *48*, 1642−1667.
(8) Schmidt, D. J.; Moskowitz, J. S.; Hammond, P. T. Electrically Triggered Release of a Small Molecule Drug from a Polyelectrolyte Multilayer Coating. *Chem. Mater.* **2010**, *22*, 6416−6425.
(9) Hoffman, A. S. Hydrogels for biomedical applications. *Adv. Drug Delivery Rev.* **2012**, *64*, 18−23.
(10) Caló, E.; Khutoryanskiy, V. V. Biomedical applications of hydrogels: A review of patents and commercial products. *Eur. Polym. J.* **2015**, *65*, 252−267.
(11) Lorenzo, R. A.; Carro, A. M.; Concheiro, A.; Alvarez-Lorenzo, C. Stimuli-responsive materials in analytical separation. *Anal. Bioanal. Chem.* **2015**, *407*, 4927−4948.
(12) Szunerits, S.; Teodorescu, F.; Boukherroub, R. Electrochemically triggered release of drugs. *Eur. Polym. J.* **2016**, *83*, 467−477.
(13) Vidinha, P.; Lourenço, N. M. T.; Pinheiro, C.; Brás, A. R.; Carvalho, T.; Santos-Silva, T.; Mukhopadhyay, A.; Romão, M. J.; Parola, J.; Dionisio, M.; Cabral, J. M. S.; Afonso, C. A. M.; Barreiros, S. Ion jelly: a tailor-made conducting material for smart electrochemical devices. *Chem. Commun.* **2008**, 5842−5844.
(14) Borisova, O. V.; Billon, L.; Richter, R. P.; Reimhult, E.; Borisov, O. V. pH- and Electro-Responsive Properties of Poly(acrylic acid) and Poly(acrylic acid)-*block*-poly(acrylic acid-*grad*-styrene) Brushes Studied by Quartz Crystal Microbalance with Dissipation Monitoring. *Langmuir* **2015**, *31*, 7684−7694.
(15) Dias, A. M. A.; Cortez, A. R.; Barsan, M. M.; Santos, J. B.; Brett, C. M. A.; de Sousa, H. C. Development of Greener Multi-Responsive Chitosan Biomaterials Doped with Biocompatible Ammonium Ionic Liquids. *ACS Sustainable Chem. Eng.* **2013**, *1*, 1480−1492.
(16) Chen, J.; Gao, L-. x.; Han, X.; Chen, T.; Luo, J.; Liu, K.; Gao, Z.; Zhang, W. Preparation and electro-response of chitosan-*g*-poly(acrylic acid) hydrogel elastomers with interpenetrating network. *Mater. Chem. Phys.* **2016**, *169*, 105−112.
(17) Jayaramudu, T.; Ko, H.-U.; Kim, H. C.; Kim, J. W.; Li, Y.; Kim, J. Transparent and semi-interpenetrating network P(vinyl alcohol)-P(Acrylic acid) hydrogels: pH responsive and electroactive application. *Int. J. Smart Nano Mater.* **2017**, *8*, 80−94.
(18) Li, Y.; Zhang, C.; Zhou, Y.; Dong, Y.; Chen, W. Novel multi-responsive polymer materials: When ionic liquids step in. *Eur. Polym. J.* **2015**, *69*, 441−448.
(19) Mecerreyes, D. Polymeric ionic liquids: Broadening the properties and applications of polyelectrolytes. *Prog. Polym. Sci.* **2011**, *36*, 1629−1648.
(20) Huber, B.; Rossrucker, L.; Sundermeyer, J.; Roling, B. Ion transport properties of ionic liquid-based polyelectrolytes. *Solid State Ionics* **2013**, *247−248*, 15−21.
(21) Leones, R.; Sabadini, R. C.; Esperança, J. M. S. S.; Pawlicka, A.; Silva, M. M. Playing with ionic liquids to uncover novel polyelectrolytes. *Solid State Ionics* **2017**, *300*, 46−52.
(22) Egorova, K. S.; Gordeev, E. G.; Ananikov, V. P. Biological Activity of Ionic Liquids and Their Application in Pharmaceutics and Medicine. *Chem. Rev.* **2017**, *117*, 7132−7189.
(23) Chen, J.; Xie, F.; Li, X.; Chen, L. Ionic liquids for the preparation of biopolymer materials for drug/gene delivery: a review. *Green Chem.* **2018**, *20*, 4169−4200.
(24) Javed, F.; Ullah, F.; Zakaria, M. R.; Akil, H. Md. An approach to classification and hi-tech applications of room-temperature ionic liquids (RTILs): A review. *J. Mol. Liq.* **2018**, *271*, 403−420.
(25) Berthod, A.; Ruiz-Ángel, M. J.; Carda-Broch, S. Recent advances on ionic liquid uses in separation techniques. *J. Chromatogr. A* **2018**, *1559*, 2−16.
(26) Liu, H.; Yu, H. Ionic liquids for electrochemical energy storage devices applications. *J. Mater. Sci. Technol.* **2019**, *35*, 674−686.
(27) Zhao, Q.; Chu, H.; Zhao, B.; Liang, Z.; Zhang, L.; Zhang, Y. Advances of ionic liquids-based methods for protein analysis. *TrAC, Trends Anal. Chem.* **2018**, *108*, 239−246.
(28) Sasikumar, B.; Arthanareeswaran, G.; Ismail, A. F. Recent progress in ionic liquid membranes for gas separation. *J. Mol. Liq.* **2018**, *266*, 330−341.
(29) Shaplov, A. S.; Marcilla, R.; Mecerreyes, D. Recent Advances in Innovative Polymer Electrolytes based on Poly(ionic liquid)s. *Electrochim. Acta* **2015**, *175*, 18−34.
(30) Qian, W.; Texter, J.; Yan, F. Frontiers in poly(ionic liquid)s: syntheses and applications. *Chem. Soc. Rev.* **2017**, *46*, 1124−1159.
(31) Muñoz-Bonilla, A.; Fernández-García, M. Poly(ionic liquid)s as antimicrobial materials. *Eur. Polym. J.* **2018**, *105*, 135−149.
(32) Chen, M.; White, B. T.; Kasprzak, C. R.; Long, T. E. Advances in phosphonium-based ionic liquids and poly(ionic liquid)s as conductive materials. *Eur. Polym. J.* **2018**, *108*, 28−37.
(33) Nulwala, H.; Mirjafari, A.; Zhou, X. Ionic liquids and poly(ionic liquid)s for 3D printing - A focused mini-review. *Eur. Polym. J.* **2018**, *108*, 390−398.
(34) Lee, C.-P.; Ho, K.-C. Poly(ionic liquid)s for dye-synthesized solar cells: A mini-review. *Eur. Polym. J.* **2018**, *108*, 420−428.
(35) Delhorbe, V.; Bresser, D.; Mendil-Jakani, H.; Rannou, P.; Bernard, L.; Gutel, T.; Lyonnard, S.; Picard, L. Unveiling the Ion Conduction Mechanism is Imidazolium-Based Poly(ionic liquids): A Comprehensive investigation of the Structure-to-Transport Interplay. *Macromolecules* **2017**, *50*, 4309−4321.
(36) Salas-De la Cruz, D.; Green, M. D.; Ye, Y.; Elabd, Y. A.; Long, T. E.; Winey, K. I. Correlating backbone-to-backbone distance to

DOI: 10.1021/acssuschemeng.9b01071
ACS Sustainable Chem. Eng. 2019, 7, 10516−10532

ionic conductivity in amorphous polymerized ionic liquids. *J. Polym. Sci., Part B: Polym. Phys.* **2012**, *50*, 338−346.
(37) Alemán, J. V.; Chadwick, A. V.; He, J.; Hess, M.; Horie, K.; Jones, R. G.; Kratochvíl, P.; Meisel, I.; Mita, I.; Moad, G.; Penczek, S.; Stepto, R. F. T. Definition of terms relating to the structure and processing of sols, gels, networks, and inorganic-organic hybrid materials (IUPAC Recommendations 2007). *Pure Appl. Chem.* **2007**, *79*, 1801−1829.
(38) Lohani, A.; Singh, G.; Bhattacharya, S. S.; Verma, A. Interpenetrating Polymer Networks as Innovative Drug Delivery Systems. *J. Drug Delivery* **2014**, *2014*, 1−11.
(39) Dragan, E. S. Design and applications of interpenetrating polymer network hydrogels. A review. *Chem. Eng. J.* **2014**, *243*, 572−590.
(40) Becht, G. A.; Sofos, M.; Seifert, S.; Firestone, M. A. Formation of a Liquid-Crystalline Interpenetrating Poly(Ionic liquid) Network Hydrogel. *Macromolecules* **2011**, *44*, 1421−1428.
(41) Shaplov, A. S.; Ponkratov, D. O.; Vlasov, P. S.; Lozinskaya, E. I.; Gumileva, L. V.; Surcin, C.; Morcrette, M.; Armand, M.; Aubert, P.-H.; Vidal, F.; Vygodskii, Y. S. Ionic semi-interpenetrating networks as a new approach for highly conductive and stretchable polymer materials. *J. Mater. Chem. A* **2015**, *3*, 2188−2198.
(42) Juger, J.; Vancaeyzeele, C.; Plesse, C.; Nguyen, G. M. T.; Braz Ribeiro, F.; Teyssié, D.; Vidal, F. Polymeric Ionic liquid based interpenetrating polymer network for all-solid self-standing polyelectrolyte material. *Eur. Polym. J.* **2018**, *106*, 257−265.
(43) Tudor, A.; Florea, L.; Gallagher, S.; Burns, J.; Diamond, D. Poly(Ionic Liquid) Semi-Interpenetrating Network Multi-Responsive Hydrogel. *Sensors* **2016**, *16*, 219.
(44) Vilela, C.; Sousa, N.; Pinto, R. J. B.; Silvestre, A. J. D.; Figueiredo, F. M. L.; Freire, C. S. R. Exploiting poly(ionic liquids) and nanocellulose for the development of bio-based anion-exchange membranes. *Biomass Bioenergy* **2017**, *100*, 116−125.
(45) Zhang, C.; Zhang, W.; Gao, H.; Bai, Y.; Sun, Y.; Chen, Y. Synthesis and gas transport properties of poly(ionic liquid) based semi-interpenetrating polymer network membranes for CO_2/N_2 separation. *J. Membr. Sci.* **2017**, *528*, 72−81.
(46) Elvira, C.; Mano, J. F.; San Román, J.; Reis, R. L. Starch-based biodegradable hydrogels with potential biomedical applications as drug delivery systems. *Biomaterials* **2002**, *23*, 1955−1966.
(47) Salgado, A. J.; Coutinho, O. P.; Reis, R. L. Novel starch-based scaffolds for bone tissue engineering: Cytotoxicity, cell culture and protein expression. *Tissue Eng.* **2004**, *10*, 465−474.
(48) Li, Y.; Tan, Y.; Xu, K.; Lu, C.; Wang, P. A biodegradable starch hydrogel synthesized via thiol-ene click chemistry. *Polym. Degrad. Stab.* **2017**, *137*, 75−82.
(49) Dalton, P. D.; Shoichet, M. S. Creating porous tubes by centrifugal forces for soft tissue application. *Biomaterials* **2001**, *22*, 2661−2669.
(50) Willems, N.; Yang, H.-y.; Langelaan, M. L. P.; Tellegen, A. R.; Grinwis, G. C. M.; Kranenburg, H.-J. C.; Riemers, F. M.; Plomp, S. G. M.; Craenmehr, E. G. M.; Dhert, W. J. A.; Papen-Botterhuis, N. E.; Meij, B. P.; Creemers, L. B.; Tryfonidou, M. A. Biocompatibility and intradiscal application of a thermoreversible celecoxib-loaded poly-N-isopropylacrylamide MgFe-layered double hydroxide hydrogel in a canine model. *Arthritis Res. Ther.* **2015**, *17*, 1−16.
(51) Sinha, M.; Gupte, T. Design and evaluation of artificial cornea with core-skirt design using polyhydroxyehtyl methacrylate and graphite. *Int. Ophthalmol.* **2018**, *38*, 1225−1233.
(52) Hernandez-Martínez, A. R.; Lujan-Montelongo, J. A.; Silva-Cuevas, C.; Mota-Morales, J. D.; Cortez-Valadez, M.; Ruíz-Baltazar, A. J.; Cruz, M.; Herrera-Ordonez, J. Swelling and methylene blue adsorption of poly(*N, N*-dimethacrylamide-*co*-2-hydroxyethyl methacrylate) hydrogel. *React. Funct. Polym.* **2018**, *122*, 75−84.
(53) Salmieri, S.; Khan, R. A.; Safrany, A.; Lacroix, M. Gamma rays-induced 2-hydroxyehtyl methacrylate graft copolymerization on methylcellulose-based films: Structure analysis and physicochemical properties. *Ind. Crops Prod.* **2015**, *70*, 64−71.
(54) Al-Mohammed, N. N.; Alias, Y.; Abdullah, Z. Bis-imidazolium and benzimidazolium based gemini-type ionic liquid structure: synthesis and antibacterial evaluation. *RSC Adv.* **2015**, *5*, 92602−92617.
(55) Cavoue, T.; Abassi, H. B.; Vayssade, M.; Nguyen Van Nhien, A.; Kang, I.-K.; Kwon, G.-W.; Porceau, G.; Dubot, P.; Andaloussi, S. A.; Versace, D.-L. Imidazolium-based titanium substrates against bacterial colonization. *Biomater. Sci.* **2017**, *5*, 561−569.
(56) Kizil, R.; Irudayaraj, J.; Seetharaman, K. Characterization of Irradiated Starches by Using FT-Raman and FTIR Spectroscopy. *J. Agric. Food Chem.* **2002**, *50*, 3912−3918.
(57) Worzakowska, M. Starch-g-poly(benzyl methacrylate) copolymers. *J. Therm. Anal. Calorim.* **2016**, *124*, 1309−1318.
(58) Talu, M.; Demiroğlu, E. U.; Yurdakul, Ø.; Badoğlu, S. FTIR, Raman and NMR spectroscopy and DTF theoretical studies on poly(N-vinylimidazole). *Spectrochim. Acta, Part A* **2015**, *134*, 267−275.
(59) Hsueh, Y.-H.; Liaw, W.-C.; Kuo, J.-M.; Deng, C.-S.; Wu, C.-H. Hydrogel Film-Immobilized *Lactobacillus brevis* RK03 for γ-Aminobutyric Acid Production. *Int. J. Mol. Sci.* **2017**, *18*, 2324−2337.
(60) Drozdov, A. D.; deClaville Christiansen, J. Swelling of pH-sensitive hydrogels. *Phys. Rev. E* **2015**, *91*, 1−15.
(61) Dodoo, S.; Steitz, R.; Laschewsky, A.; von Klitzing, R. Effect of ionic strength and type of ions on the structure of water swollen polyelectrolyte multilayers. *Phys. Chem. Chem. Phys.* **2011**, *13*, 10318−10325.
(62) Ganguly, S.; Maity, T.; Mondal, S.; Das, P.; Das, N. C. Starch functionalized biodegradable semi-IPN as a pH-tunable controlled release platform for memantine. *Int. J. Biol. Macromol.* **2017**, *95*, 185−198.
(63) Kaur, L.; Singha, J.; Liu, Q. Starch - A potential biomaterial for biomedical applications. In *Nanomaterials and Nanosystems for Biomedical Applications*; Mozafari, M. R., Ed.; Springer: The Netherlands, 2007; pp 83−98, DOI: 10.1007/978-1-4020-6289-6_5.
(64) Dragan, E. S.; Apopei, D. F. Multiresponsive macroporous semi-IPN composite hydrogels based on native or anionically modified potato starch. *Carbohydr. Polym.* **2013**, *92*, 23−32.
(65) Dragan, E. S.; Apopei Loghin, D. F.; Cocarta, A.-I.; Doroftei, M. Multi-stimuli-responsive semi-IPN cryogels with native and anionic potato starch entrapped in poly (N, N-dimethylaminoethyl methacrylate) matrix and their potential in drug delivery. *React. Funct. Polym.* **2016**, *105*, 66−77.
(66) Restolho, J.; Mata, J. L.; Colaço, R.; Saramago, B. Moisture Absorption in Ionic Liquid Films. *J. Phys. Chem. C* **2013**, *117*, 10454−10463.
(67) Brovchenko, I.; Oleinikova, A. Effect of Pore Size on the Condensation/Evaporation Transition of Confined Water in Equilibrium with Saturated Bulk Water. *J. Phys. Chem. B* **2011**, *115*, 9990−10000.
(68) Czepirski, L.; Komorowska-Czepirska, E.; Szymońska, J. Fitting of different models for water vapour sorption on potato starch granules. *Appl. Surf. Sci.* **2002**, *196*, 150−153.
(69) Worthley, C. H.; Constantopoulos, K. T.; Ginic-Markovic, M.; Pillar, R. J.; Matisons, J. G.; Clarke, S. Surface modification of commercial cellulose acetate membranes using surface-initiated polymerization of 2-hydroxylehtyl methacrylate to improve membrane surface biofouling resistance. *J. Membr. Sci.* **2011**, *385*−*386*, 30−39.
(70) Pineda-Gómez, P.; Angel-Gil, N.; Valencia-Muñoz, C.; Rosales-Rivera, A.; Rodríguez-García, M. E. Thermal degradation of starch sources: Green banana, potato, cassava and corn - kinetic study by non-isothermal procedures. *Starch* **2014**, *66*, 691−699.
(71) Khoonsap, S.; Narkkun, T.; Ratphonsan, P.; Klinsrisuk, S.; Amnuaypanich, S. Enhancing the grafting of poly(2-hydroxyehtyl methacrylate) on silica nanoparticles (SiO_2-*g*-HEMA) by the sequential UV-induced graft polymerization with a multiple-UV irradiation. *Adv. Powder Technol.* **2014**, *25*, 1304−1310.
(72) Ulu, A.; Koytepe, S.; Ates, B. Synthesis and characterization of biodegradable pHEMA-starch composites for immobilization of L-asparaginse. *Polym. Bull.* **2016**, *73*, 1891−1907.

DOI: 10.1021/acssuschemeng.9b01071
ACS Sustainable Chem. Eng. 2019, 7, 10516−10532

(73) Karpushkin, E.; Dušková-Smrčková, M.; Šlouf, M.; Dušek, K. Rheology and porosity control of poly(2-hydroxyehtyl methacrylate) hydrogels. *Polymer* **2013**, *54*, 661−672.
(74) Meakin, J. R.; Hukins, D. W. L.; Aspden, R. M.; Imrie, C. T. Rheological properties of poly(2-hydroxyethyl methacrylate) (pHEMA) as a function of water content and deformation frequency. *J. Mater. Sci.: Mater. Med.* **2003**, *14*, 783−787.
(75) Barbucci, R. *Hydrogels Biological Properties and Applications*; Springer-Verlag: Mailand, Italy, 2009.
(76) Khan, M.; Schuster, S.; Zharnikov, M. Effect of Humidity on Electrical Conductivity of Pristine and Nanoparticle-Loaded Hydrogel Nanomembranes. *J. Phys. Chem. C* **2015**, *119*, 14427−14433.
(77) Ye, Y.-S.; Rick, J.; Hwang, B.-J. Ionic liquid polymer electrolytes. *J. Mater. Chem. A* **2013**, *1*, 2719−2743.
(78) Dias, A. M. A.; Marceneiro, S.; Johansen, H. D.; Barsan, M. M.; Brett, C. M. A.; de Sousa, H. C. Phosphonium ionic liquids as greener electrolytes for poly(vinyl chloride)-based ionic conducting polymers. *RSC Adv.* **2016**, *6*, 88979−88990.
(79) Cai, J.; Wei, W.; Hu, X.; Wood, D. A. Electrical conductivity models in saturated porous media: A review. *Earth-Sci. Rev.* **2017**, *171*, 419−433.
(80) Kim, O.; Kim, S. Y.; Lee, J.; Park, M. J. Building Less Tortuous Ion-Conduction Pathways Using Block Copolymers Electrolytes with a Well-Defined Cubic Symmetry. *Chem. Mater.* **2016**, *28*, 318−325.
(81) Eftekhari, A.; Saito, T. Synthesis and properties of polymerized ionic liquids. *Eur. Polym. J.* **2017**, *90*, 245−272.
(82) Soares, B. G. Ionic liquid: A smart approach for developing conducting polymer composites. *J. Mol. Liq.* **2018**, *262*, 8−18.
(83) Haleem, J. D. Improving therapeutics in anorexia nervosa with tryptophan. *Life Sci.* **2017**, *178*, 87−93.
(84) Kishimoto, N.; Katayama, Y.; Kato, M.; Otsu, H. Technical feasibility of UV/electro-chlorine advanced oxidation process and pH response. *Chem. Eng. J.* **2018**, *334*, 2363−2372.
(85) Yang, X.; Bing, T.; Mei, H.; Fang, C.; Cao, Z.; Shangguan, D. Characterization and application of a DNA aptamer binding to L-tryptophan. *Analyst* **2011**, *136*, 577−585.
(86) Xie, Y.; Jing, K.-J.; Lu, Y. Kinetics, equilibrium and thermodynamic studies of L-tryptophan adsorption using a cation exchange resin. *Chem. Eng. J.* **2011**, *171*, 1227−1233.
(87) Pérez-Martínez, C. J.; Morales Chávez, S. D.; del Castillo-Castro, T.; Ceniceros, T. E. L.; Castillo-Ortega, M. M.; Rodríguez-Félix, D. E.; Gálvez Ruiz, J. C. Electroconductive nanocomposite hydrogel for pulsatile drug release. *React. Funct. Polym.* **2016**, *100*, 12−17.
(88) Kerkaert, B.; Mestdagh, F.; Cucu, T.; Aedo, P. R.; Ling, S. Y.; De Meulenaer, B. Hypochlorous and peracetic acid induced oxidation of dairy proteins. *J. Agric. Food Chem.* **2011**, *59*, 907−914.
(89) Palza, H.; Zapata, P. A.; Angulo-Pineda, C. Electroactive Smart Polymers for Biomedical Applications. *Materials* **2019**, *12*, 277.
(90) Pairatwachapun, S.; Paradee, N.; Sirivat, A. Controlled release of acetylsalicylic acid from polythiophene/carrageenan hydrogel via electrical stimulation. *Carbohydr. Polym.* **2016**, *137*, 214−221.
(91) Patinha, D. J. S.; Alves, F.; Rebelo, L. P. N.; Marrucho, I. M. Ionic liquid aqueous biphasic systems: Effect of the alkyl chains in the cation versus the anion. *J. Chem. Thermodyn.* **2013**, *65*, 106−112.
(92) Tomé, L. I. N.; Catambas, V. R.; Teles, A. R. R.; Freire, M. G.; Marrucho, I. M.; Coutinho, J. A. P. Tryptophan extraction using hydrophobic ionic liquids. *Sep. Purif. Technol.* **2010**, *72*, 167−173.
(93) Capela, E. V.; Quental, M. V.; Domingues, P.; Coutinho, J. A. P.; Freire, M. G. Effective separation of aromatic and aliphatic amino acid mixtures using ionic-liquid-based aqueous biphasic systems. *Green Chem.* **2017**, *19*, 1850−1854.
(94) Amde, M.; Liu, J.-F.; Pang, L. Environmental Application, Fate, Effects, and Concerns of Ionic Liquids: A Review. *Environ. Sci. Technol.* **2015**, *49*, 12611−12627.
(95) Xia, Y.; Liu, D.; Dong, Y.; Chen, J.; Liu, H. Effect of ionic liquids with different cations and anions on photosystem and cell structure of Scenedesmus obliquus. *Chemosphere* **2018**, *195*, 437−447.
(96) Liu, H.; Zhang, X.; Chen, C.; Du, S.; Dong, Y. Effects of imidazolium chloride ionic liquids and their toxicity to Scenedesmus obliquus. *Ecotoxicol. Environ. Saf.* **2015**, *122*, 83−90.
(97) Bacon, L. S.; Ross, R. J.; Daugulis, A. J.; Parent, J. S. Imidazolium-based polyionic liquid absorbents for bioproduct recovery. *Green Chem.* **2017**, *19*, 5203−5213.
(98) Filipović, V. V.; Nedeljković, B. B.; Vukomanović, M.; Tomić, S. Lj. Biocompatible and degradable scaffolds based on 2-hydroxyehtyl methacrylate, gelatin and poly(beta amino ester) crosslinkers. *Polym. Test.* **2018**, *68*, 270−278.
(99) Vraneš, M.; Tot, A.; Javonović-Šanta, S.; Karaman, M.; Dožić, S.; Tešanović, K.; Kojić, V.; Gadžurić, S. Toxicity reduction of imidazolium-based ionic liquids by the oxygenation of the alkyl substituent. *RSC Adv.* **2016**, *6*, 96289−96295.
(100) Täuber, K.; Lepenies, B.; Yuan, J. Polyvinylpyridinium-type gradient porous membranes: synthesis, actuation and intrinsic cell growth inhibition. *Polym. Chem.* **2015**, *6*, 4855−4858.
(101) Marques, A. P.; Pirraco, R. P.; Reis, R. L. Biocompatibility of starch-based polymers. In *Natural-Based Polymers for Biomedical Applications*; Reis, R. L., Neves, N. M., Mano, J. F., Gomes, M. E., Marques, A. P., Azevedo, H. S., Eds.; Woodhead Publishing Series in Biomaterials, 2008; pp 738−760, DOI: 10.1533/9781845694814.6.738.
(102) Balmayor, E. R.; Baran, T. E.; Unger, M.; Marques, A. P.; Azevedo, H. S.; Reis, R. L. Presence of starch enhances *in vitro* biodegradation and biocompatibility of a gentamicin delivery formulation. *J. Biomed. Mater. Res., Part B* **2015**, *103*, 1610−1620.

DOI: 10.1021/acssuschemeng.9b01071
ACS Sustainable Chem. Eng. 2019, 7, 10516−10532

Supporting information

Sustainable electro-responsive semi-interpenetrating starch/ionic liquid copolymer networks for the controlled sorption/release of biomolecules

Akel F. Kanaan[1], Madalina M. Barsan[2], Christopher M.A. Brett[2], Carmen Alvarez-Lorenzo[3], Angel Concheiro[3], Hermínio C. de Sousa[1], Ana M.A. Dias[1*]*

[1]CIEPQPF, Chemical Engineering Department, FCTUC, University of Coimbra, Pólo II, 3030-790 Coimbra, Portugal
[2]Chemistry Department, FCTUC, University of Coimbra, Rua Larga, 3004-535 Coimbra, Portugal
[3]Department of Pharmacology, Pharmacy and Pharmaceutical Technology, R+D Pharma Group (GI-1645), Faculty of Pharmacy, University of Santiago de Compostela, 15782 Santiago de Compostela, Spain

*Corresponding authors: adias@eq.uc.pt and hsousa@eq.uc.pt

Number of pages: 6

Number of figures: 4

Number of tables: 1

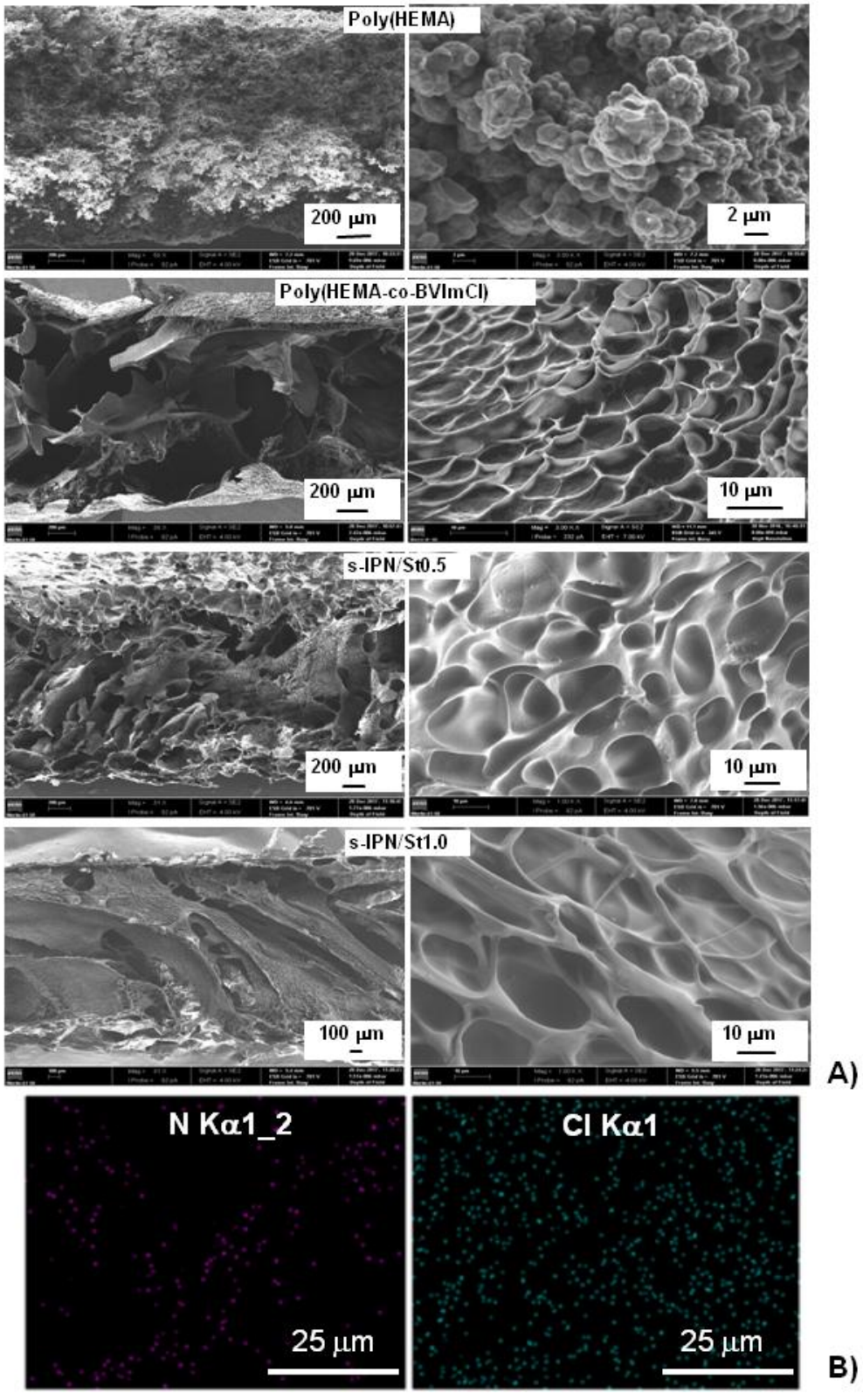

Figure S1. Cross-section SEM micrographs of freeze-dried hydrogels (A) and elemental mapping of nitrogen and chlorine distribution through the hydrogel s-IPN/St1.0, analyzed by energy dispersive X-ray spectroscopy (EDX) (B). Similar EDX results were obtained for hydrogels poly(HEMA-co-BVImCl) and s-IPN/St0.5.

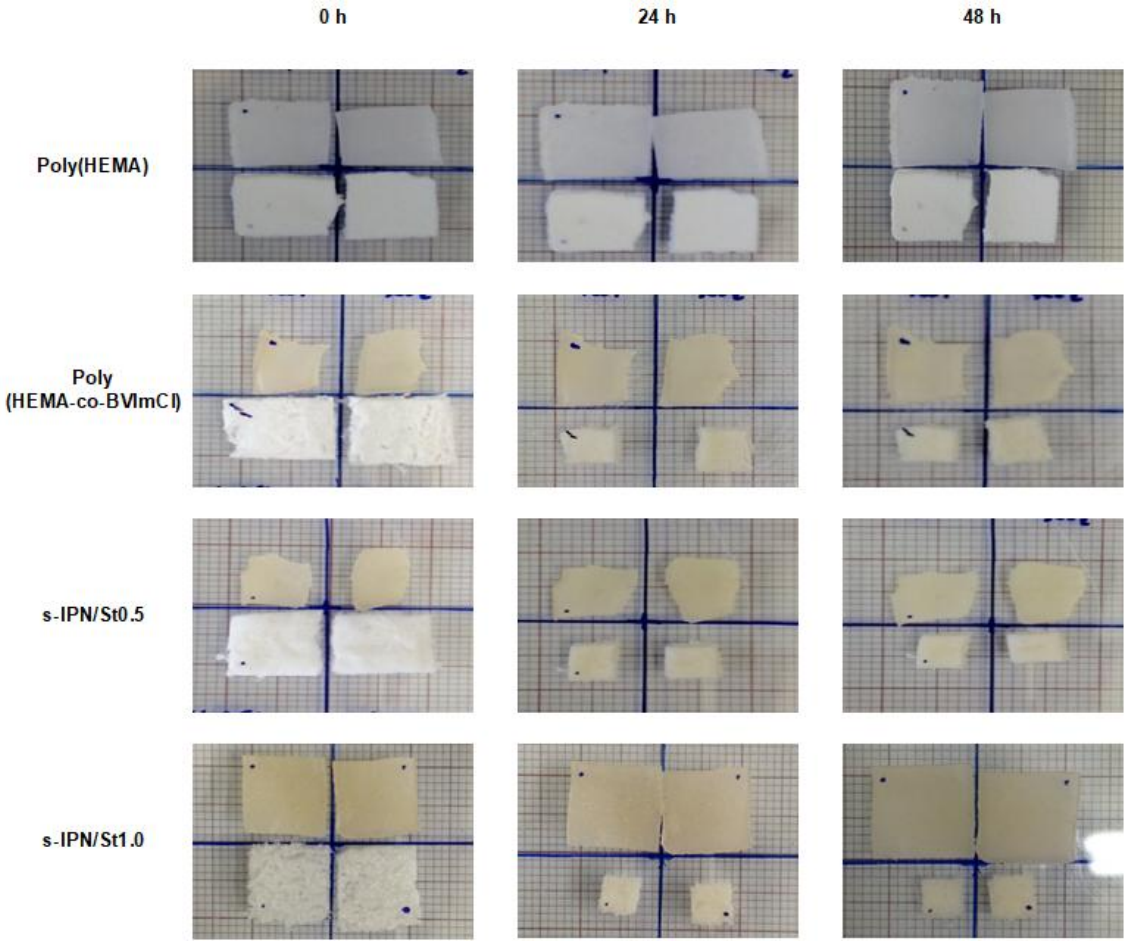

Figure S2. Mechanical response of oven- and freeze-dried hydrogels (upper and lower samples in each figure, respectively) during WVS measurements at RH ≥ 90% and 25 ^{o}C.

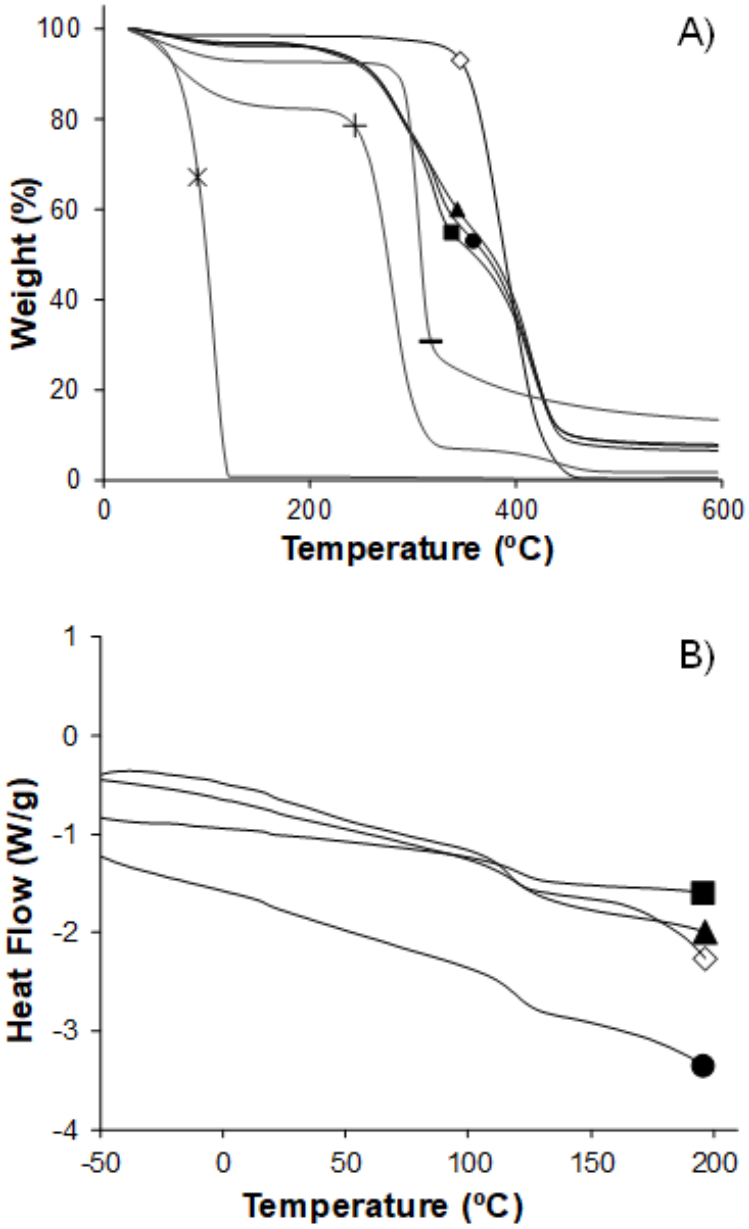

Figure S3. Thermogravimetric profiles (A) and DSC thermograms (B) of the hydrogels (Exothermal events oriented up). The symbols represent: poly(HEMA) (◊), poly(HEMA-co-BVImCl) (●), s-IPN/St0.5 (▲), s-IPN/St1.0 (■). The thermogravimetric profiles of pure HEMA (✕), BVImCl (+) and starch (—) are also shown for comparison.

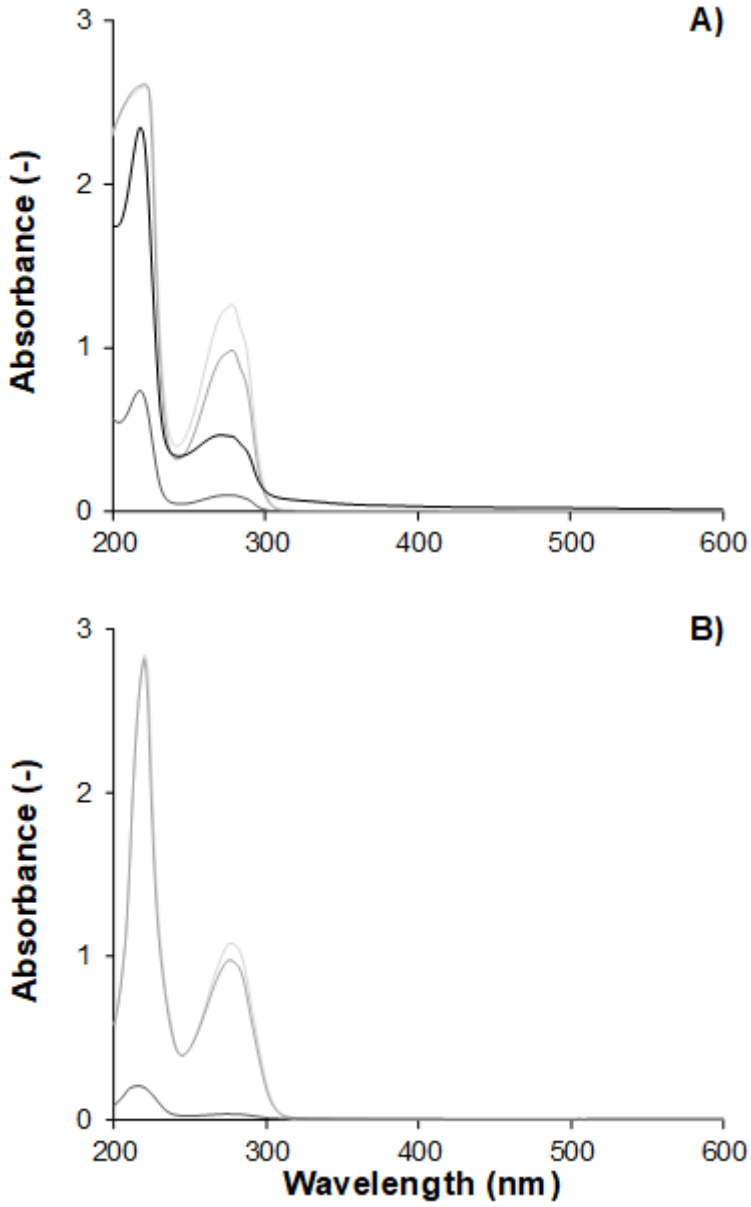

Figure S4. Spectra of L-tryptophan solutions in bi-distilled water (A) and in Trizma base buffer (B) after electro-assisted sorption experiments at 0 V (—), 2 V (—), 5 V (—) and 100 V (—) at room temperature (~ 25 ºC).

Table S1. Average values (% w/w) of nitrogen, carbon, hydrogen and sulfur content of prepared hydrogels obtained from elemental analysis (after washing the hydrogels).

	N % (w/w)	C % (w/w)	H % (w/w)	S % (w/w)
Poly(HEMA)	0.07 ± 0.02	53.14 ± 0.15	8.08 ± 0.03	≤ 100 ppm
Poly(HEMA-co-BVImCl)	2.73 ± 0.27	53.14 ± 0.15	8.07 ± 0.07	≤ 100 ppm
s-IPN/St0.5	2.61 ± 0.45	53.18 ± 0.03	8.11 ± 0.10	≤ 100 ppm
s-IPN/St1.0	3.03 ± 0.02	52.70 ± 0.40	8.04 ± 0.03	≤ 100 ppm

Note: the experimental amount of BVImCl per weight of dry sample was calculated as follows (using the sample s-IPN/St1.0 as an example):

Basis: 100 g of s-IPN/St1.0 sample has an average of 3.03 g of nitrogen atoms (N) which correspond to 0.2164 mol of N.

1) Each molecule of BVImCl has 2 N atoms in their chemical structure (in the cation). Therefore the number of moles of BVImCl is half that of the N atoms: 0.108 mol of BVImCl (per 100 g of dried sample).

2) The experimental amount of BVImCl per weight of dry sample was expressed in Table 1 as:

$$\frac{\text{BVImCl (mmol)}}{\text{100 g of dried sample s-IPN/St1.0}} = 1.082 \text{ mmol BVImCl/g of dried sample.}$$